Max-Planck-Institut
für Meteorologie

REPORT No. 201

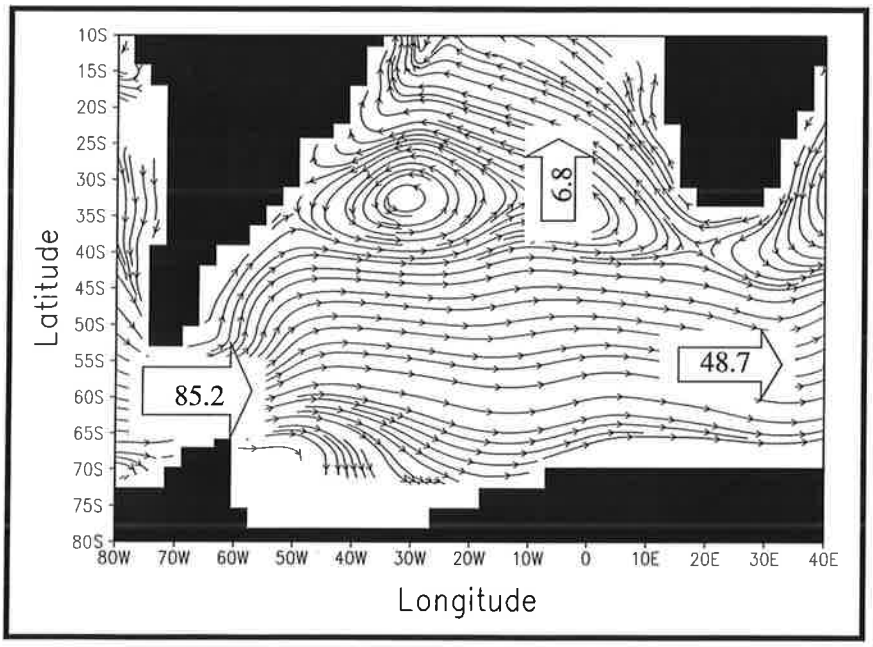

INTERPRETATION OF INTERBASIN EXCHANGE IN AN ISOPYCNAL OCEAN MODEL

by

Xue-Hong Zhang • Josef M. Oberhuber • Andreas Bacher • Erich Roeckner

HAMBURG, July 1996

AUTHORS:

Xue-Hong Zhang:
Institute of Atmospheric Physics
Chinese Academy of Sience
Beijing
China
E-Mail: zxh@lasgsgi8.iap.ac.cn

Josef M. Oberhuber:
Deutsches Klimarechenzentrum GmbH
Hamburg
F. R. Germany

Andreas Bacher,
Erich Roeckner:
Max-Planck-Institute for Meteorology
Hamburg
F. R. Germany

MAX-PLANCK-INSTITUT
FÜR METEOROLOGIE
BUNDESSTRASSE 55
D-20146 HAMBURG
F.R. GERMANY

Tel.: +49 - (0)40 - 411 73 - 0
Telefax: +49 - (0)40 - 411 73 - 298
E-Mail: <name>@dkrz.de

ISSN 0937 – 1060

Interpretation of Interbasin exchange in an Isopycnal Ocean Model

Xue-Hong Zhang*, Josef M. Oberhuber, Andreas Bacher, Erich Roeckner**

Max-Planck Institute for Meteorology
Bundesstrasse 55, D-20146 Hamburg, Germany

(Submitted for publication in *Climate Dynamics*)

(July, 1996)

ISSN 0937 - 1060

---

* Current affiliation: State Key Laboratory of Numerical Modelling for Atmospheric Sciences and Geophysical Fluid Dynamics, Institute of Atmospheric Physics, Chinese Academy of Sciences, P.O.Box 2718, Beijing 100080, China. (e-mail: zxh@lasgsgi8.iap.ac.cn)

** Deutsches Klimarechenzentrum GmbH

Abstract

This paper reports an analysis of interbasin and inter-layer exchanges in the component ocean part of the coupled ECHAM4/OPYC3 general circulation model, aimed at documenting the simulation of North Atlantic Deep Water (NADW) and related thermohaline circulations in the Indian and Pacific Oceans. The modeled NADW is formed mainly in the Greenland-Iceland-Norwegian Seas through a composite effect of deep convection and downward cross-isopycnal transport. The modeled deep-layer outflow of NADW can reach 16 Sv near 30°S in the South Atlantic, with the corresponding upper-layer return flow mainly coming from the "cold water path" through Drake Passage. Less than 4 Sv of the Agulhas "leakage" water contribute to the replacement of NADW along the "warm water path". In the South Atlantic Ocean, the model shows that some intermediate isopycnal layers with potential densities ranging between 27.0 and 27.5 are the major water source for compensating the NADW return flow and for enhancing the Circumpolar Deep Water (CDW) flowing from the Atlantic into Indian Ocean. The modeled thermohaline circulations in the Indian and Pacific Oceans indicate that the Indian Ocean may play the major role in converting deep water into intermediate water. About 16 Sv of the CDW-originating deep water enter the Indian Ocean northward of 31°S, of which more than 13 Sv "upwell" mainly near the continental boundaries of Africa, South Asia and Australia through inter-layer exchanges and return to the Antarctic Circumpolar Current (ACC) as intermediate-layer water. As a contrast, only 4 Sv of Pacific intermediate water connected to "upwelling" flow southward across 31°S while the magnitude of northward deep flow across 31°S in the Pacific Ocean is significantly greater than that in the Indian Ocean. The model suggests that a large portion of the deep waters entering the Pacific Ocean (about 14 Sv) "upwells" continually into some upper layers through the thermocline, and becomes the source of the Indonesian throughflow. Uncertainties in these results may be related to the incomplete adjustment of the model's isopycnal layers and the sensitivity of the Indonesian throughflow to the model's geography and topography.Abstract

1. Introduction

The world ocean's thermohaline circulation (or "conveyor belt" as first introduced by Broecker (1987, 1991)) has been presumed to be important for understanding the linkages among the elements of the Earth's climate system. Traditionally, studies of the thermohaline circulation have focused on the formation of North Atlantic Deep Water (NADW). In recent years, however, the path and process of the renewal of NADW is becoming another attractive topic due to their close connection with the interbasin and inter-layer exchanges of various water masses in the world ocean.

It is generally accepted that there are two branches of return path of NADW outflow i.e. the "warm water path" and "cold water path" (Gordon, 1986, Broecker, 1991). Concerning the partitioning of these two return paths, while being a controversial issue (e.g. see Rintoul, 1991), the results given by various authors are now getting more and more consistent. That is, about 10 Sv (1 Sv = 10^6 m^3 s^{-1}) of intermediate water enters the South Atlantic Ocean via Drake Passage along the "cold water path", and the amount of "warm water" transport from the South Indian Ocean to Atlantic Ocean around the southern tip of Africa is about 4 Sv (Gordon et al., 1992, Schmitz, 1995). However the process in which deep water is eventually converted to upper-layer water is still poorly understood. In fact, the prototypes of both the "warm water path" and "cold water path" schemes were established on the basis of a two-layer framework in which the exchange between the lower and upper limbs of the conveyor belt takes place in a rather straight way. Consequently, some broad-area uniform upwelling through thermocline must be assumed to link up the lower and upper limbs (Gordon, 1986), which perhaps could only be regarded as a zero-order approximation to the upward transport associated with the conveyor belt.

As demonstrated by Rintoul (1991) in his inverse calculation based on hydrographic data that the global thermohaline circulation cell started from the formation and export of NADW is closed primarily by the "cold water path" in which deep water leaving the Atlantic ultimately returns as intermediate water entering the basin through Drake Passage. And, as a whole, the South Atlantic

converts intermediate water into deep and bottom waters. It is a logical inference that NADW leaving the Atlantic should be converted to intermediate water somewhere before reentering the basin. Therefore one can expect that further investigations of conversion from deep water to intermediate water would improve our understanding about "upwelling" branches of the global-scale thermohaline circulation.

Toole and Warren (1993) calculated transports across the section along 32°S in the Indian Ocean based on data from a full-depth observation. They obtained a figure for the net transport of water below 2000m of 27 Sv northward, which implies an average upwelling speed at 2000m level north of 32°S of 6 cm day^{-1}. With the associated calculations of heat and fresh water flux divergences, they suggested that the Indian Ocean thermohaline circulation essentially expresses a conversion of bottom and deep water to mid-depth thermocline water, and near-surface water. In their study, the estimate of net southward transport of intermediate water across 32°S is about 10 Sv. Meanwhile, with an inverse calculation based on data from six hydrographic basinwide sections in the three major basins, Macdonald (1993) obtained a similar estimate of the net southward transport of intermediate water across 32°S in the Indian Ocean (about 9 Sv). The magnitude of net northward transport of deep and bottom water estimated in her study is strongly controlled by the priori estimate of the Indonesian Passage throughflow (IT): 21 Sv without IT, and 13 Sv and 5 Sv corresponding to the magnitude of IT of 10 Sv and 20 Sv respectively (see Macdonald, 1993, Table 9). From 32°S to 18°S, the northward transport of deep and bottom water even becomes slightly stronger, implying that the major "upwelling" from deep water to intermediate water in the Indian Ocean could take place north of 18°S or even further northward.

A comprehensive review on the interbasin-scale thermohaline circulation was presented by Schmitz recently (Schmitz, 1995). By piecing together published observational results, he suggested a four-layer scheme for the global-scale thermohaline circulation, of which the layers were defined in terms of their potential density ranges. The potential density of his "upper" layer is less than 26.8 kg m^{-3} (σ_θ units hereinafter are understood). For his "intermediate", "upper deep", and

"lower deep and bottom" layers, the potential density ranges are σ_θ~26.8-27.5, σ_θ~27.6-27.7, and σ_θ~27.8-28.1 respectively. Based on results reported by Toole and Warren (1993) and Macdonald (1993), Schmitz speculated that about 10 Sv of the intermediate water converted from the northward flowing deep and bottom water in the Indian Ocean could be the most important source for NADW compensation along the "cold water path" (see Plate 7, or 9 and 10, in his paper).

Ocean modelling has made considerable progress in recent years in approaching overall representations of the world ocean's thermohaline circulation. A variety of ocean-only models or coupled ocean-atmosphere models can simulate, to certain extent, the formation of NADW (Bryan & Lewis, 1979; Manabe et al., 1991; Semtner & Chervin, 1992; England, 1993; Maier-Reimer et al., 1993; Oberhuber, 1993b; Zhang et al., 1995) although the intensities of NADW and the overall structures of the global-scale conveyor belt in these simulations are significantly model-dependent. Meanwhile, sensitivities of the simulated thermohaline circulation to various factors including geography and bottom topography, surface forcing (heat and fresh water fluxes), mixing parameterization, horizontal and vertical resolutions, etc. have been a very important aspect in modelling activities (Bryan, 1986; Cox, 1989; England, 1993; Maier-Reimer et al., 1993, S.Zhang et al., 1993).

As to the process of NADW's renewal, only a few modelling results were published so far. The eddy-resolving model of Semtner and Chervin (1992) suggests that of the 14 Sv of NADW outflow in their model, 6 Sv or more returns through an Indonesian warm water route and up to 6 Sv along a cold route. It was found in their model that the deep circulation rises towards the surface in a series of switchbacks mainly in the equatorial Pacific. In the Hamburg Large Scale Geostrophic (LSG) model of Maier-Reimer, Mikolajewicz and Hasselmann (1993), a two-layer picture of the conveyor belt was depicted, of which the return flow of NADW is almost completely through Drake Passage, and the upwelling from the lower ocean (below 1500m depth level) to upper ocean (above 1500m) occurs mainly in equatorial regions in the Pacific and Indian Oceans (see Figure 1 in their paper). They also mentioned that the transport from the Pacific

Ocean to Indian Ocean through the Indonesian Passage is very sensitive to the representation of topography in the Banda Strait between Indonesia and Australia. In one of a series of sensitivity experiments with the GFDL model, England (1993) found that the Indonesian Passage throughflow mainly served to redistribute the barotropic flow, and little response was detected in the global meridional overturning. Recently, England and Garcon (1994) analyzed mass exchanges among thermocline, intermediate and deep waters in the South Atlantic within a global z-coordinates ocean model with 33 levels. In order to identify the three types of water mass, following Gordon et al. (1992), they defined the thermocline water as water warmer than 9°C, intermediate water be cooler than 9°C but shallower than 1500m, and deep water being below 1500m. Their analysis shows a partitioning between the cold water route through Drake Passage (6.5 Sv), and the warm water route involving the Agulhas Current shedding thermocline water westward (2.5 Sv) and a recirculation of intermediate water originating in the Indian Ocean (1.6 Sv).

In this paper, we will report an analysis of inter-basin and inter-layer exchanges in a multi-layer isopycnal ocean model (Oberhuber 1992) as used in a coupled general circulation model (GCM) simulation of present-day climate involving an atmospheric GCM (Roeckner et al. 1996, Bacher et al. 1996). Isopycnal models are based on the concept that buoyancy forces in a stratified fluid may influence flow and mixing to conserve density more than other characteristics. Although the assumption of maximum mixing and flow along isopycnal surfaces remains an assumption (Reid, 1981), it has been accepted as an useful concept in distinguishing water masses with different properties especially in the subsurface ocean where the characteristics of water masses are highly conservative. One of the advantages of using an isopycnal model in studying interbasin exchange is that upper, intermediate, deep and bottom waters can be approximately represented by using some existing layers of the model (or their combinations), with specific potential density ranges, without need of alternative definitions. Meanwhile, in a multi-layer isopycnal model, the water-mass "modification" or "conversion" (Schmitz, 1995) can be explicitly expressed by using parameterized inter-layer exchange processes, e.g. entrainment/detrainment or diapycnal mixing

(see Oberhuber, 1993a). Recognizing that observational data are not sufficient and reliable enough to depict the thermohaline circulation particularly in the Pacific and Indian Oceans and, a validation of ocean models, covering both surface and subsurface layers, is not available so far, we intended to present a conceptual diagram for interpreting some interesting aspects concerning mainly the renewal of NADW rather than a detailed picture of thermohaline circulation. Thus some simplified analyses aimed at documenting the modeled NADW and relevant circulations in the Indian and Pacific Oceans have been performed based on a data set describing a representative state of the model's control integration. The emphasis of this paper will be put on the conversion from deep layer circulation to intermediate layer circulation and associated water mass transports among the three major basins, without including analyses of water mass property conversion or modification. Moreover, no attempt was made in this study to investigate interannual and interdecadal variabilities of the modeled thermohaline circulation in this study although the ocean-atmosphere coupled model has exhibited such variabilities.

A brief introduction to the isopycnal ocean model and the associated coupled system is given in section 2. Section 3 describes the modeled NADW, its outflow and return flow in the Atlantic basin, which represent the central part of the conveyor belt but are not closed in this single basin. In order to lead the discussion to interbasin and inter-layer exchanges, an analysis of the water mass budget in the South Atlantic Ocean southward of 31°S is given in section 4. An interpretation of the thermohaline circulation in the Indian Ocean northward of 31°S is presented in Section 5, which demonstrates the role of the Indian Ocean in converting deep water to intermediate water. Section 6 discusses the meridional and vertical transports in the Pacific Ocean northward of 31°S, and their uncertainties. The main conclusions are summarized in section 7.

2. Model description

The ocean model is the OPYC (Ocean isoPYCnal) general circulation model developed by Oberhuber (1992, 1993a). It solves the primitive equations in the form of conservation laws for

momentum, mass, heat and salt in isopycnal layers, with a realistic state equation of sea water. A mixed layer is included as the top layer with an arbitrary potential density and a minimum thickness of 10 m. The elevation of the sea surface is given by vertical summation of layer thicknesses which vary in space and time. Diapycnal and isopycnal mixing are parameterized respectively, using a Richardson-number dependent criterion and Laplacian diffusion with temporally and spatially varying coefficients. The latter for momentum depends on local Rossby-radius, for scalars on the local deformation of flow field. The convective adjustment completely removes vertical instability in each timestep. A dynamic-thermodynamic sea-ice model is incorporated with sea-ice dynamics based on that of Hibler (1979).

The horizontal spatial discretization is on a B-grid (Arakawa and Lamb, 1977) with scalar points on a T42 Gaussian grid as used in some spectral atmospheric models except equatorward of 36^{o} latitude where the meridional spacing is gradually decreased to approximately 0.5^{o} to resolve the equatorial wave guide. The model has 11 layers including the mixed layer. A semi-implicit method is used in the model's time-integration with a time step of half a day. In uncoupled simulations, surface fluxes are given by bulk laws involving observed climatological atmospheric quantities and simulated surface temperature (Oberhuber, 1988, 1993a), and surface salinity forcing includes Haney (1971)-type restoring in addition to precipitation and evaporation.

For spinning up the ocean model, approximately 1000 years of ocean-only integration were conducted. The first 500 years used monthly mean observed climatology as input to the surface flux parameterizations except taking the windstress from an uncoupled integration of ECHAM3 AGCM (Roeckner et al., 1992). Subsequently, day-to-day variability of total heat flux and precipitation minus evaporation anomalies from ECHAM3 was added.

The isopycnal ocean model was used in a coupled GCM simulation at the Max Planck Institute for Meteorology (MPI) involving the fourth generation MPI AGCM, ECHAM4 (Roeckner et al. 1996, Bacher et al. 1996). Each day, averages of windstress, net heat and freshwater fluxes,

river discharge, downward solar radiation and turbulent kinetic energy flux are delivered by the AGCM which in turn is forced by SST and sea ice/snow cover from the ocean model. As described in Bacher and Oberhuber (1996), net freshwater flux and heat flux (or ice melting/freezing rate as computed in the AGCM) are adjusted by adding spatially varying but time-independent annual mean correlations. This is done to counter climate drift which coupled GCMs commonly develop from startup if no measures are taken to account for either component model tending to a separate equilibrium in uncoupled mode (see also Sausen et al. 1988, Manabe & Stouffer 1991). The data used in this study are taken from year 120 to 150 out of a total of 250 simulation years.

Figure 1 shows the zonal mean layer distribution in the Atlantic Ocean, calculated based on the layer-thickness data averaged from the year 120 to 150. Unlike z-coordinate model, the layer thicknesses in an isopycnal model are not uniformly distributed particularly in high latitudes where the steep slopes of isopycnals are favorable to the exchange between surface and subsurface waters. Some small-scale fluctuations of layer-interfaces (particularly for some lower layers) can be found near the equator in this figure, which are obviously related to the use of small latitudinal grid-sizes in the equatorial region. To simplify layer analyses and develop a conceptual diagram of the interbasin and inter-layer exchanges, we first combined the 11 layers to form 3 layers: upper, intermediate and deep layers. The upper layer consists of the layers 1-6 of which the potential densities are less than 26.7 kg m^{-3}. The intermediate layer consists of the layers 7, 8 and 9 with the potential densities ranging between 27.0 and 27.5. The deep layer includes the layer 10 and 11 with the potential densities of 27.6 and 27.7 (strictly speaking, the layer 11 is not an isopycnal, but it can roughly keep the potential density value through inter-layer exchanges). The definition of the three combined layers used here is similar to that of Schmitz (1995) although the model does not include the "lower deep and bottom" layer as described in Schmitz's scheme. In the following, these three layers will be called "UL", "ML", and "DL". The layer variables include potential temperature θ, salinity S, water mass content ρh, and water mass fluxes ρhu and

ρhv, where ρ is in-situ density, h is layer-thicknesses, and u and v are velocity components along longitudinal and latitudinal directions respectively.

$$\frac{\partial}{\partial t}(\rho h)_k + \nabla\bullet(\rho h\vec{v})_k - \Delta(w\rho)_k^{k+1} + \Delta(w\rho)_{k-1}^{k} = 0 \qquad (1)$$

In estimating inter-layer exchanges, the mass content equation (Eq.(1)) was used as a diagnostic equation rather than a prognostic equation. There are three sorts of terms in Eq.(1). The first one is the local change of the mass content, and the second one is the mass-flux divergence dependent on not only the velocity divergence and the spatial variation of density, which are also included in z-coordinate models, but also the spatial variations of layer thickness, which may characterize thickness distributions of various water masses. The third sort of terms are the net water mass transport from the adjacent lower layer (layer k+1) to this specific layer (layer k) and that from the layer k to its adjacent upper layer (layer k-1) respectively. The "net" transport from layer k+1 to layer k is referred here as the difference between the entrainment from layer k+1 into layer k and the detrainments from layer k into layers k+1. For the first layer (k=1), the "net" transport to its "upper" layer should be interpreted as an upward fresh water flux through the surface.

The net water mass transport from layer k+1 to layer k can be determined based on Eq.(1) of which the mass divergence term can be calculated simply with the model's horizontal mass-flux data, the corrected fresh water flux is available as one of the quantities exchanged between the ocean model and the atmospheric model, and the local change term can be estimated based on the layer-thickness changes within the 30 years of the model's integration. All these terms have an unit of kg s^{-1}. For the sake of convenience conventionally, all the mass transports have been transformed into volume transports. Thus the unit used in the following for describing both the interbasin and inter-layer transports will be Sverdrup (Sv, 1 Sv=10^6 m^3/s). In an isopycnal model, the inter-layer exchange is essentially involved in the water mass conversion or modification rather than large-scale advective process. The terminology of "upwelling" and "downwelling", which will be used in the followings for the sake of simplicity, should be understood as upward and

downward transports related to entrainment/detrainment or diapycnal mixing processes. Moreover, the local change term in Eq.(1) is not negligible particularly in the model's intermediate and deep layers due to changes of the layer thicknesses during the analyzed 30 years. Thus the layer-adjustment process in the current phase of the model's integration should be taken into account in interpreting interbasin exchanges.

In the following sections, components of the simulated thermohaline circulation in the three major basins will be viewed with a combination of maps of zonal mean meridional overturning streamfunction, bar charts for flow amount through some selected meridional and zonal sections, and vector streamline plots of mass fluxes in the three major basins.

3. Atlantic overturning

Figure 2 shows the meridional overturning streamfunction in the Atlantic basin restricted to the region north of 30°S (again, some small-scale fluctuations found in the equatorial region are related to the small meridional grid sizes there). Since our major concern in this study is the global-scale thermohaline circulation of which the central part is North Atlantic Deep Water (NADW), we simply interpolated velocity components from the 11 isopycnal layers into 48 evenly-spaced levels in the z-coordinate to calculate the overturning streamfunction. Due to the use of relatively coarse vertical resolution near the surface, some shallow wind-driven Ekman cells which have been simulated successfully with this model are filtered out from this figure. On the other hand, no advective traces of Antarctic Bottom Water (AABW) can be found from this figure. As mentioned in section 2, the model does not include layers matched to the lower deep layer and bottom layer in the real ocean. Some waters formed in the Ross Sea and Weddell Sea, with potential densities greater than that of the model's bottom layer, are mixed with the bottom-layer and its adjacent upper-layer waters. This limitation is mainly related to the layer-arrangement (in terms of the range of potential densities of the layers) in this low-vertical-resolution version of the OPYC model used for the coupled ECHAM4/OPYC3-run.

Apart from its overestimated vertical extension, the modeled NADW and the associated cross-equatorial outflow and upper-layer return flow in the Atlantic basin shown in Figure 2 are rather successful. The over-extending of the modeled NADW in the vertical is obviously related to the lack of the bottom water in the model as mentioned above. The modeled maximal overturning rate is about 24 Sv which seems to be in the highest end of the range of some other estimates, e.g. 15-20 Sv (Gordon, 1986), 15-25 Sv (Broecker, 1991), and 14 Sv (Schmitz, 1995). This large transport rate of the modeled NADW could be partly attributed to the layer-thickness change occurring in an incomplete adjustment process of the model. In fact, the DL is becoming thicker with a rate of 4.3 Sv in the Atlantic Ocean between 31°S and 66°N during the time period of these 30 years, and correspondingly the ML is becoming thinner with the same rate.

One of the noticeable aspects related to the modeled NADW formation is that the main "downwelling" branch near 60°N shown in Figure 2 seems to result from a composite effect of deep convection and inter-layer entrainment/detrainment processes. According to Killworth (1983), the primary sites of open-ocean convection in Northern Hemisphere are Labrador Sea, Greenland Sea, and Mediterranean Sea. In the model, convection occurs mainly in the Greenland-Iceland-Norwegian Seas. Figure 3 shows that the annual mean convective depth can reach more than 500m depth in the southeast of Greenland and more than 1000m depth in the northeast of the Iceland-Faroe Channel respectively (the maximal convective depth during wintertime can reach more than 2000m). It is believable that the comparatively strong convective activities in these areas would trigger the strong "downwelling" there. In fact, Figure 4(b) shows that the major downward transport from the ML to DL in the North Atlantic Ocean occurs in the subpolar and polar regions: about 12 Sv in 50°-60°N, 10 Sv in 60°-70°N, and 4 Sv in 70°-80°N, of which most may contribute to the NADW formation and the rest could be the source of thickness-increase of the DL. Moreover, Figure 4(a) shows that the main downward transport from the UL to ML takes place between 30°-60°N, of which the 4 Sv occurring in 50°-60°N could be related to the relatively weak convection there (see Figure 3). Combining Figure 4(a), 4(b), and Figure 2, we can

infer that a portion of these water masses "downwelled" from the UL (about 5 Sv) may further "downwell" into the DL, and the rest (about 5-6 Sv) need to flow poleward within the ML to close the mass budget of the Atlantic thermohaline cell. The inter-layer transport in the South Atlantic Ocean shown also in Figure 4(a) and (b) will be discussed in the next section.

Figure 5 shows the meridional volume transport in the DL at each grid point across the latitudes at 66°N and 31°N, and the equator in the Atlantic basin. The net equatorward transport of deep water across the Denmark Strait and Iceland-Faroe Channel at 66°N is about 6 Sv. Most of this overflow from the polar sea enters subpolar sea through the Iceland-Faroe Channel (Figure 5(a)) probably because of the major site of deep convection being in the northeast of Iceland. The overflow entrains a large amount of intermediate water from the ML-to-DL transport around the latitudes of 50°-70°N as shown in Figure 4(b) and reaches its maximal intensity of 24 Sv around the latitudes of 30°-40°N (see Figure 2). Meanwhile it shifts from the eastern side of the basin, in high latitudes, to the western side in low latitudes, particularly in a zone along the western continental boundary (see Figure 5(b)), and develops gradually as the model's DWBC (Deep Western Boundary Current). This can be seen even more clearly from the longitudinal distribution of the cross-equatorward transport of deep water shown in Figure 5(c) where the total magnitude of the DWBC-like current between 32°W and 43°W can reach more than 28 Sv while the net transport across the equator is only 18-19 Sv due to the existence of recirculation in the equatorial region (see Figure 6, the vector streamlines in the DL). Between 31°N and the equator, more than 3 Sv of deep water "upwell" into the ML (see Figure 4(b)), then flow poleward and return to the northern North Atlantic eventually as shown in Figure 2.

The meridional transports across 31°S in the South Atlantic basin are shown in Figure 7(a-c) for the layers of UL, ML, and DL respectively. The net southward volume transport across 31°S in the DL is 16.1 Sv of which about two third is carried by the DWBC-like current located in the west of 30°W and the rest is transported along the path in the east of the Mid-Atlantic Ridge (see Figure 7(c)). These southward deep currents represent the modeled NADW outflow which can be

clearly seen in Figure 6. Meanwhile, in the layers UL and ML, the dominant transports are northward (see Figure 7(a) and (b)) which correspond to the NADW return flow within the upper 1500m range shown in Figure 2. A calculation shows that the net northward transport across 31°S are 8.4 Sv in the UL and 6.8 Sv in the ML respectively. About 0.9 Sv of the difference between the southward deep flow and northward upper-layer and intermediate-layer flows across the section of 31°S is balanced by the inflow of equal magnitude from the North Pacific into the Arctic through the Bering Strait. The modeled Pacific-to-Arctic transport of 0.9 Sv through the Bering Strait is quite close to a recent estimation of 0.77 Sv given by Wijffels et al. (1992).

It is found from Figure 7 that the southward flow can extend from the UL through ML to DL along the western boundary, and the equatorward flow is almost limited to the two upper layers and located mainly in the eastern part of the basin. This reflects some characteristics of the large-scale circulation in the South Atlantic. The poleward flow may be divided into two currents: the Brazil Current in the upper layers, corresponding to the western boundary current of the South Atlantic subtropical gyre (see Figure 8(a-b)), and the DWBC-like deep current associated with the thermohaline circulation, shown in Figure 6. The circulation patterns for the UL and ML are rather similar, but they are remarkably different from the circulation for the DL. In fact, the "DWBC" in the DL turns to south-eastward or eastward flow after leaving the western boundary between 30°-45°S, and joins the Circumpolar Deep Water (CDW) without any significant northward component in the Atlantic basin. On the other hand, however, the western boundary currents in the two upper layers represent only a segment of the subtropical gyre of which the recirculation associated with the Benguela Current is the major contributor to the return flow of NADW.

4. South Atlantic water mass budget

The South Atlantic Ocean has been regarded as a key region for the global-scale thermohaline circulation due in part to its open connections with the North Atlantic, South Indian, and South Pacific Oceans. The NADW outflow is exported to the Indian and Pacific Oceans and the return

flow is imported from the two oceans through interbasin exchanges. In order to gain an insight into the interbasin exchanges, we start from an analysis of the water mass budget within the South Atlantic poleward of 31°S, a region with three open boundaries at 31°S, 70°W (Drake Passage) and 20°E respectively. Based on Eq.(1), the components of the budget, as listed in Table 1, include the water mass flux convergence (or divergence) resulting from the imported water offset by the exported water through the open boundaries, the net entrainment (or detrainment) from (or into) the adjacent upper and lower layers, and the mass deficit (or surplus) due to the change of layer thickness.

In the UL, the inflow from the South Pacific through Drake Passage into the South Atlantic is 9.4 Sv, and the outflow from the South Atlantic into the South Indian Ocean across 20°E is 8.7 Sv. In addition to these imported and exported flows along the Antarctic Circumpolar Current (ACC), there is an equatorward flow of 8.4 Sv out of the region crossing 31°S as aforementioned. Such an area-integral of water flux divergence results in a volume deficit of 7.7 Sv for the UL in this region. On the other hand, the layer's total volume in this region has only a little change (0.02 Sv). Thus the deficit must be compensated by an upward transport from the underlying ML, and perhaps, plus the fresh-water flux imported from the atmosphere. Since the amount of the net surface fresh water flux over this region is negligible, the source for balancing this 7.7 Sv of water deficit can only be sought from the ML.

In fact, Figure 4 has already shown that the ML in the Atlantic Ocean southward of 31°S is the water source for not only the UL but also the DL because of a large amount of water mass flux convergence in this region. Up to 85.2 Sv of the ML-water is imported from the South Pacific through Drake Passage into the South Atlantic, which accounts for more than two thirds of the total transport of ACC (the transports of the modeled ACC across the sections at Drake Passage and at 20°E are 107.7 Sv and 108.6 Sv respectively). On the other hand, the total amount of the ML-water exported from this region is only 55.5 Sv of which 48.7 Sv flows into the Indian Ocean through the section of 20°E and 6.8 Sv flows equatorward crossing 31°S as a portion of the

NADW return flow. Thus the ML-water convergence in this region is up to 29.7 Sv. Moreover, the layer-volume in this region is decreasing with a rate of 2.2 Sv which provides an additional source for the inter-layer exchanges but represents essentially the contribution of layer-adjustment process. An equilibrium calculation based on Eq.(1) shows that the ML may provide 7.7 Sv to the UL and 24.2 Sv to DL to compensate their volume divergences and provide the source for the volume increase associated with layer's thickening mainly in the DL.

Figure 9 shows the horizontal distributions of the net upward water volume transport from the ML to UL (a) and from DL to ML (b). In order to depict the large-scale characteristics of these inter-layer exchanges, the fields were "upscaled" by transforming the original data into those in 32*18 boxes with sizes of 11.25 degrees in longitude and 10 degrees in latitude. It can be found from Figure 9(a) that the ML-to-UL transport in the South Atlantic Ocean southward of 31^{o}S is not uniformly distributed. For instance, about 5 Sv upward transport takes place in the western side of the region where the ACC in the upper layer mostly flows northward in the Malvinas Current, then joins the South Atlantic subtropical gyre, and eventually merges into the Benguela Current (see Figure 8(a)). This flow pattern seems to be favorable to transport the O(5 Sv) of upwelled ML-water northward to compensate the return flow of NADW. The rest of the upwelled intermediate water occurring south of 50^{o}S might not contribute directly to the replacement of NADW, instead it could compensate the ACC mass export to the South Indian Ocean in the UL.

In addition to the inflow from the Pacific into the Atlantic through Drake Passage, there are some UL and ML waters, leaked from the Agulhas Current in the Indian Ocean, entering the Atlantic via the southern tip of Africa. The southward transport of the modeled Agulhas Current across 31^{o}S is about 59 Sv consisting of 34 Sv of UL-water and 25 Sv of ML-water (see Figure 10(a) and (b)). Most of these southward flowing UL-water and ML-water turn eastward after leaving the coast of Africa between 30^{o}-40^{o}S, and join the ACC ultimately. Meanwhile, there are about 2 Sv of UL-water and less than 2 Sv of ML-water flowing westward and crossing the section at 20^{o}E, as the leakage of the Agulhas Current (see Figure 11(a) and (b)). It can be seen from

Figure 8 that this 3-4 Sv of UL and ML water (or most of them) may directly join the Benguela Current and become involved in compensating the NADW return flow along the "warm water path". Thus the model suggests that the contribution of the Indian Ocean UL and ML water to the 15.2 Sv of the return flow crossing 31°S in the Atlantic Ocean (8.4 Sv of UL-water plus 6.8 Sv of ML-water) is no more than 4 Sv, implying that more than 70% of the contribution to the replacement of NADW may come from the flow along the "cold water path" from the Pacific Ocean through Drake Passage.

Although the total transport across the section at 20°E is roughly equal to that across Drake Passage (a surplus of 0.9 Sv comes from the North Pacific UL-water through the Bering Strait), the transport in individual layers is not the same across each section. More ML-water enters the Atlantic from the Pacific than leaves to the Indian Ocean. The opposite is true for the DL where 51.2 Sv of deep water leaves for the Indian Ocean through 20°E (Figure 11 (c)), which is 22 Sv greater than the sum of the inflow from the Pacific (13.1 Sv) and the poleward NADW outflow crossing 31°S (16.1 Sv) (see Table 1). As mentioned before, the ML provides 24.2 Sv water to the DL to compensate the 22 Sv of deficit related to the flux divergence and the 2.2 Sv of volume increasing associated with the layer thickening of DL (also see Table 1). Thus the model's results support such the suggestion that the South Atlantic as a whole converts intermediate water into deep water (Rintoul, 1991). Logically, the excess of deep water exported from the South Atlantic Ocean must be converted to intermediate water (and upper-layer water) in certain places in the Indian and Pacific Oceans to feed that imported into the Atlantic through Drake Passage.

5. Thermohaline circulation in Indian Ocean

Figure 12 displays the vector streamline of mass flux in the DL in the Indian and Pacific Oceans (20°E-70°W). The modeled Circumpolar Deep Water (CDW) flows through the southern Indian and Pacific Oceans with noticeable northward components entering the two basins. It should be kept in mind that the modeled CDW, in terms of its potential density range, represents

only the deep water rather than the mixture of deep and bottom waters in the real ocean. Due to this limitation, the model can not simulate the conversion from bottom water to deep water occurring in the three major basins as described by Schmitz (1995). In the following, we will concentrate on the water mass exchange between the model's deep-layer water (DL-water) and intermediate-layer water (ML-water), and begin by discussing the CDW-originating northward flows across the sections along 31°S in the Indian Ocean.

In the DL, the net equatorward transport across 31°S in the Indian Ocean is about 16 Sv (Figure 10(c)) which is 3 Sv greater than that estimated by Macdonald (1993, Table 3, Model B) but 11 Sv less than that deduced by Toole and Warren (1993). It should be pointed out that the vertical ranges of deep water (or deep plus bottom water) used in these studies are comparable but not the same. The model's zonal mean upper boundary of the DL at 31°S in the Indian Ocean is at about 2400m depth, and the thickness of the DL is about 400m less than the vertical range of the northward transport across 30°S in the Indian Ocean estimated by Toole and Warren (1993). On the other hand, the σ_2 value (potential density with the reference pressure of 2000 dbar) of the upper boundary of the DL is roughly 36.8, quite similar to that used in Macdonald (1993). Thus the modeled O(16 Sv) of DL-water entering the Indian Ocean northward of 31°S seems to be an acceptable estimate.

Combining Figure 12 and Figure 10(c), we can find that there are three major branches of equatorward flowing current across the section along 31°S in the Indian Ocean, all of which originate from the CDW around 40°-50°S and are strongly affected by bottom topography while moving northward. Across the west portion of the section of 31°S, about 2 Sv (around 50°E) and 6 Sv (within 60°-80°E) of DL-water flow northward towards the Madagascar Basin and Central Indian Basin respectively. On the other hand, Figure 9(b) shows a strong "upwelling" region in the west of about 55°E, between 31°S and the equator, bounded to the west by Africa, and covering the Mozambique Basin and a portion of the Madagascar Basin and Somali Basin, where the net transport from the DL-water to ML-water can reach more than 5 Sv. There are some indications in Fig-

ure 12 that the major part of the 2 Sv plus 6 Sv of northward transport across the western portion of the section at 31°S could compensate this "upwelling", and the rest flows further northward, then turns westward and enters the Somali Basin, and ultimately arrives in the North Indian Ocean along the transequatorial path in the Somali Basin. Another branch of equatorward flowing current across 31°S is found within 90°-110°E (Figure 10(c)), but mainly in a rather narrow passageway in the Berth Basin bounded to the west by the Broken Plateau and to the east by the Australian continent (see Figure 12). Figure 9(b) indicates that about 3 Sv of this 8 sv of northward flow "upwells" into the ML in the Berth Basin and the eastern side of the West Australian Basin and North Australian Basin. The major part of this deep current continues to flow northward along the western side of the West and North Australian Basins, then turns westward near the equator, perhaps merges with the northward flow along the path in the Central Indian Basin, crosses the equator in the Somali Basin, and eventually spreads in the North Indian Ocean. The net cross-equatorial transport of DL-water from the South Indian Ocean to North Indian Ocean is about 5 Sv. Figure 10(d) shows that the major transequatorial passageway in the DL is in the western side of the Somali Basin (near 50°E) where more than 8 Sv of DL-water from the South Indian Ocean enter the North Indian Ocean. Also shown in Figure 10(d), some weak recirculation can be found within 55°-80°E of the section at the equator with a net southward transport of about 3 Sv. Corresponding to the cross-equatorial transport of DL-water and the associated recirculation, there is a large area of "upwelling", covering the Central Indian Basin northward of 10°S and almost the whole North Indian Ocean including the Arabian Sea and the Bay of Bengal, with the total transport of more than 5 Sv from the DL to ML (Figure 9(b)). It can also be found from Figure 9(b) that the "downwelling" from the ML to DL in the Indian Ocean northward of 31°S is very weak, with the total amount of downward transport of only 1 Sv. Summing up all the "upwelling" and "downwelling" in this region, we found that the net DL-to-ML transport in the Indian Ocean northward of 31°S reaches above 13 Sv. On the other hand, the net upward transport from the ML to UL (Figure 9(a)) in this region is only 1 Sv (correspondingly, the integral divergence of the UL in this region is very weak). Therefore, as a whole, the Indian Ocean northward

of 31°S converts deep water into intermediate-layer water. While the amplitudes of vertical transport can be clearly seen in the Figure 9(a) and 9(b), one should keep in mind that the figures can only represent some large-scale distributions of vertical transport because of using much larger grid-size than those of the model.

Since the Indian Ocean northward of 31°S is closed on the west, north and east by continental boundaries except for the Indonesian Passage which connects the Indian Ocean and Pacific Ocean within the depth range of the UL and ML, most of the "upwelled" DL-water must flow southward in the ML and leaves the region across the section of 31°S. A calculation indicates that the net southward transport in the ML across 31°S reaches about 27 Sv of which about 13 Sv originate from the DL-to-ML "upwelling" as described above, 11 Sv comes from the inflow from the Pacific Ocean into the Indian Ocean through the Indonesian Passage (see Figure 13), and 3 Sv result from the decreasing of ML-thickness. The southward return flow in the ML across the 31°S section shown in Figure 13 is chiefly concentrated in the Agulhas Current near the western boundary, along both the Mozambique Channel and the east of Madagascar, with a magnitude of about 25 Sv, while northward transport across the section in this layer is negligible as shown in Figure 10(b) (Figure 13 shows a weak anti-cyclonic circulation in the subtropical South Indian Ocean but almost completely located in the north of 31°S, without significant components crossing the 31°S section). Meanwhile, Figure 14, combined with Figure 10(a), indicates a basin-scale anti-cyclonic circulation associated with the subtropical gyre in the South Indian Ocean. In the upper layer, the southward transport in the Agulhas Current can reach 34 Sv, and the northward transport in the interior (between 60°-110°E) is about half of the southward transport (~17 Sv). Combining Figure 10 (a) and (b) we obtained a western-boundary-current-like southward transport of 59 Sv which is about 10 Sv greater than the January-July averaged Sverdrup transport estimated by Hellermann and Rosenstein (1983), but significantly less than the estimate of 85 Sv given by Toole and Warren (1993). It is interesting that while the upper branch of this "western-boundary-current" in the UL is related to the subtropical gyre in the South Indian Ocean, the lower branch in the ML seems

to be mainly related to the thermohaline circulation in the Indian Ocean. In fact, the "western-boundary-current" in the ML, after passing the 31°S section, primarily turns eastward and joins the ACC to compensate the intermediate water entering the South Pacific and South Atlantic Oceans.

The thermohaline circulation in the Indian Ocean as interpreted based on the model's results may have uncertainties in the following two aspects. First, the model indicates 11 Sv of ML-water flowing from the Pacific Ocean into Indian Ocean through the Indonesian Passage, which eventually joins the southward transport of ML-water across the 31°S section. It can not be confirmed observationally from available measurements or diagnostic calculations whether or not such a strong transport from the Pacific Ocean to Indian Ocean can occur in the intermediate-layer. Moreover, we do not know how sensitive of the modeled Indonesian throughflow to the representation of the topography and geography around the passageway between Australia and Indonesia. It seems to be necessary to examine such a sensitivity in the future development of the model. Second, the 3 Sv of ML-water loss due to the layer thickness decrease could become involved in the southward transport ultimately, indicating an impact of the adjustment of isopycnal layers on the modeled thermohaline circulation. Regardless of these uncertainties, among the 27 Sv of southward transport across 31°S, 13 Sv come from the net upward transport from the DL to ML, which seems to be an acceptable estimate in comparison with those of Toole and Warren (1993) and Macdonald (1993) as discussed above. Perhaps more importantly, the model supports such a suggestion as discussed by Toole and Warren (1993) i.e., the Indian Ocean converts the deep water imported from the CDW to the intermediate water returning the ACC, just opposite of the North Atlantic in which thermocline water is converted to deep water.

6. Meridional and vertical transports in Pacific Ocean

Different from the South Indian Ocean where the northward deep flows are found in several separate basins, in the South Pacific Ocean, the primary northward deep flow originates from the

Southwestern Pacific basin between the dateline and 150°W where the modeled CDW is steered northward by the East Pacific Rise and split into two branches: one continue to flow eastward towards Drake Passage, the other flows northwest first and then turns northward in the east of dateline (Figure 12). The net northward transport of the DL-water across the section along 31°S in the South Pacific Ocean can reach more than 32 Sv, mainly concentrated in a rather narrow passageway within 180°-165°W (Figure 15(c)). While the magnitude of the northward transport is significantly greater than other estimates (e.g. 12 Sv given by Wunsch et al. (1983), and 10-20 Sv estimated by Schmitz (1995)), the net upward transport from the DL-water to ML-water in the Pacific Ocean northward of 31°S is about 18 Sv which accounts for only 56% of the northward transport across 31°S. The excess of the DL-water entering the Pacific Ocean northward of 31°S is balanced by the thickness increase of the DL in this region, of which the rate is up to 14 Sv. Again, this represents the impact of an adjustment process of the model's isopycnal layers on the simulated thermohaline circulation, which should be taken into account in estimating the strength of each individual component of the thermohaline circulation. For instance, the net eastward transport in the DL from the Pacific Ocean into Atlantic Ocean through Drake Passage is only 13 Sv which is likely underestimated in comparison with the corresponding value of about 40 Sv given by Rintoul (1991) and about 50 Sv given by England and Garcon (1994), in spite of some differences in the definitions of deep water used in these studies. It is apparent that the underestimation of the DL-water flowing eastward is closely related to the overestimation of the northward transport of the DL-water of which more than 40% contributes to the thickness increase of the DL in the Pacific Ocean northward of 31°S. Thus, it is speculated that the reason for the underestimated Pacific-to-Atlantic DL-water transport could be partly attributed to the incomplete adjustment process of the model's isopycnal layers.

Figure 9 shows that the areas of "upwelling" both from the DL to ML (Figure 9(b)) and from the ML to UL (Figure 9(a)) in the Pacific Ocean northward of 31°S are dispersed almost all over the region. Calculations indicate that the net transports from the DL to ML and from the ML to

UL in this region are about 18 Sv and 14 Sv respectively. These results may imply that the North Pacific Ocean converts most of the "upwelled" DL-water into UL-water and a relatively small amount (about 4 Sv) of the DL-water into ML-water. In fact, by comparing Figure 9(a) with Figure 9(b), some areas can be found in the Pacific Ocean northward of 31°S, where the DL-water can "upwell" through the thermocline and be continually converted into the ML-water and UL-water (some overlapping of the DL-to-ML and ML-to-UL "upwelling" areas can also be found in the Indian Ocean, but as indicated in the last section, the net ML-to-UL transports is much less than the transport from the DL to ML in the Indian Ocean). As a consequence, the net southward transport of ML-water across 31°S in the Pacific Ocean (Figure 15(b)) is remarkably less than that in the Indian Ocean. A water mass budget calculation shows that about 8 Sv of ML-water is exported from the north of 31°S in the Pacific Ocean, of which 4 Sv comes from the DL-to-ML transport and another 4 Sv results from the ML-thickness decrease. If we ignore the components related to the layer thickness changes, then the ratio of the southward transport across 31°S in the Pacific and Indian Oceans will be 24:4 (with the ML-water throughflow across the Indonesian Passage), or 13:4 (without the throughflow). Therefore, in any case, the Indian Ocean converts much more deep water into intermediate water to compensate the return flow of NADW than the Pacific Ocean does. In this sense, the model's results support the suggestion of Schmitz (1995) i.e. about 10 Sv of CDW converted to intermediate water in the Indian Ocean is perhaps the most important source for NADW compensation along the cold water path.

Figure 9(b) indicates comparatively strong upward transport from the DL to ML in the Philippine Basin, just northeast of the Indonesian Passage, where the DL-to-ML "upwelling" rate approximates to 3 Sv. As shown in Figure 13, it is through the Philippine Basin that a branch of rather strong southward current (about 11 Sv), connected to a basin-scale cyclonic circulation in the ML in the tropical North Pacific, enters the Indian Ocean and eventually joins the Agulhas Current to compensate the intermediate water of the ACC as described in section 5. The integral lateral divergence in the ML in the Pacific Ocean northward 31°S is about 19 Sv consisting 8 Sv

of transport to the south of 31°S and 11 Sv of transport to the Indian Ocean through the Indonesian Passage. This divergence is balanced by 4 Sv of vertical convergence (18 Sv of DL-to-ML transport minus 14 Sv of ML-to-UL transport) and about 15 Sv of the ML-thickness decrease. Thus, there seem to be greater uncertainties in the estimated lateral ML-water transports in the Pacific Ocean than those in the Indian Ocean because of the dominance of the ML-thickness decrease in the layer's water mass budget.

The UL-water exchanges between the Pacific Ocean and Indian Ocean and between the north and south of 31°S of the Pacific Ocean can be seen in Figure 14. The UL-water transport from the Pacific Ocean to Indian Ocean through the Indonesian Passage is about 15 Sv which is an acceptable approximation to the Indonesian Throughflow transport (Macdonald, 1993). Another outflow exported to the Arctic Sea through the Bering Strait is 0.9 Sv. On the other hand, the net inflow of UL-water coming from the south of 31°S is less than 3 Sv (Figure 15(a)). Thus the integral divergence in the UL in the Pacific Ocean northward of 31°S is up to 13 Sv, resulting mainly from the outflow through the Indonesian Passage. The water budget calculation shows that this divergence should be compensated primarily by the 14 Sv of vertical transport from the ML to UL, which is obviously different from the UL in the Indian Ocean northward of 31°S, where both the integral UL-divergence and the ML-to-UL transports are very weak.

7. Summary

An analysis of interbasin and inter-layer exchanges in the component ocean model of the coupled ECHAM4/OPYC3 GCM has been performed focused on water mass transports associated with the renewal of NADW. The main results of the analysis can be summarized as follows,

1) Among O(15 Sv) of the return flow of NADW, less than 4 Sv comes directly from the Indian Ocean along the "warm water path". Thus the model supports the dominance of the "cold water path" in the renewal of NADW.

2) Water mass budget analyses show that as a whole, the Indian and Pacific Oceans convert deep-layer water to intermediate-layer and upper-layer waters, just opposite of the Atlantic Ocean where intermediate-layer and upper-layer waters are converted to deep water.

3) A contrast between thermohaline circulations in the Indian and Pacific Oceans, interpreted based on inter-layer and interbasin transports, has revealed that the Indian Ocean may be the major source for the intermediate-layer water compensating the return flow of NADW along the cold water path, while a large portion of the deep water entering the Pacific Ocean may become the source of the Indonesian throughflow.

In order to further clarify the major difference between the Indian Ocean and Pacific Ocean, which has been discussed in the section 6, the latitudinal distributions of vertical transports in the north of 31^{o}S for the two basins are given in Figure 16 and 17. While "upwellings" are dominant in both basins, a strong vertical convergence in the ML can be found in the Indian Ocean (Figure 16 (b), (a)), which is sharply distinct from the picture in the Pacific Ocean where the DL-water may continually "upwells" into the UL through the ML in most of the latitudes (Figure 17(b), (a)). That is why the Indian Ocean (rather than the Pacific Ocean) plays the major role in converting deep water into intermediate water in this model.

Acknowledgments

Prof. Dr. Lennart Bengtsson's continual encouragement and valuable suggestions throughout the course of this work are highly acknowledged. This research was supported by the project 'Klimavariabilität und Signalanalyse' of the Bundesminister für Bildung und Forschung (BMBF) under grant 07VKV01/1.

This work was done during Xue-Hong Zhang's visit at Max-Planck Institute for Meteorology in Hamburg. He wishes to thank many colleagues at MPI and the German Climate Computing Centre for technical support and discussions. He also appreciates very helpful interactions with his colleagues in the Institute of Atmospheric Physics, Chinese Academy of Sciences during this time period.

TABLE 1. Water volume budget of South Atlantic poleward of 31°S (Sv).

Layer	UL	ML	DL
Area-integral convergence	*-7.7*	*29.7*	*-22.0*
Loss due to layer thinning	-0.0	2.2	-2.2
Gain from upper layer	-0.0	-7.7	24.2
Gain from lower layer	7.7	-24.2	---

For UL, "gain from upper layer" should be replaced by surface fresh water flux.

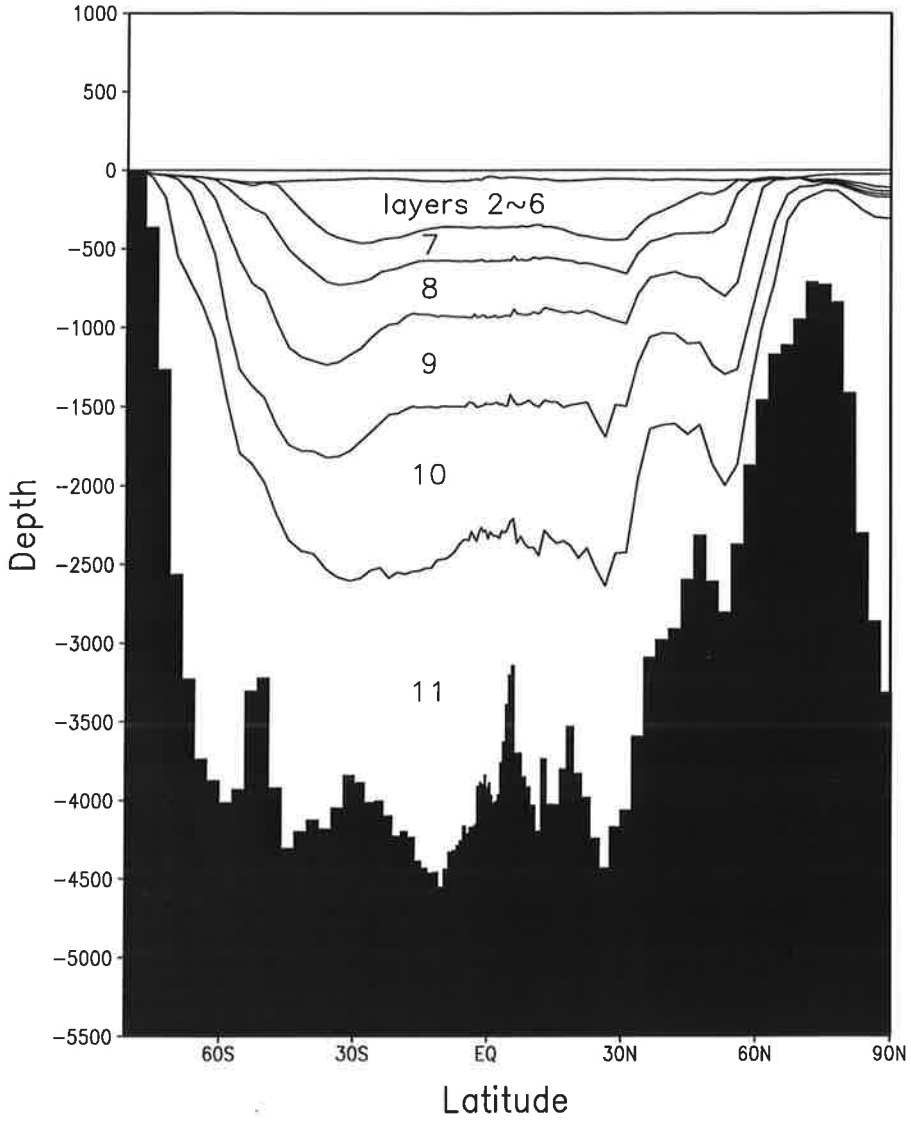

Fig. 1. Zonally averaged isopycnal layers in the Atlantic basin. The σ_θ values are 27.04, 27.30, 27.48, 27.59, and 27.71 (kg m^{-3}) for the layer 7,8,9,10,and 11 respectively, and less than 26.8 for the layers 2-6. The uppermost layer (layer 1) is the mixed layer with spatially and temporarily varying σ_θ.

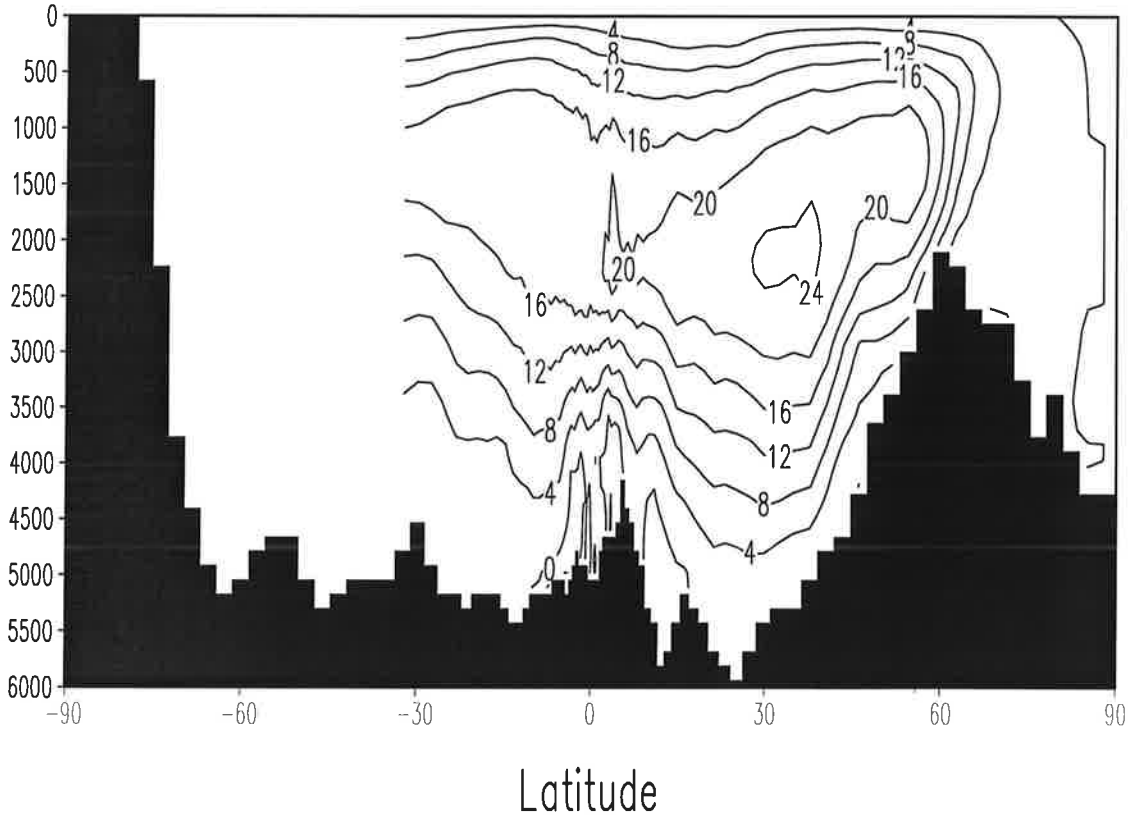

Fig. 2. Meridional overturning streamfunction (Sv) for the Atlantic Ocean.

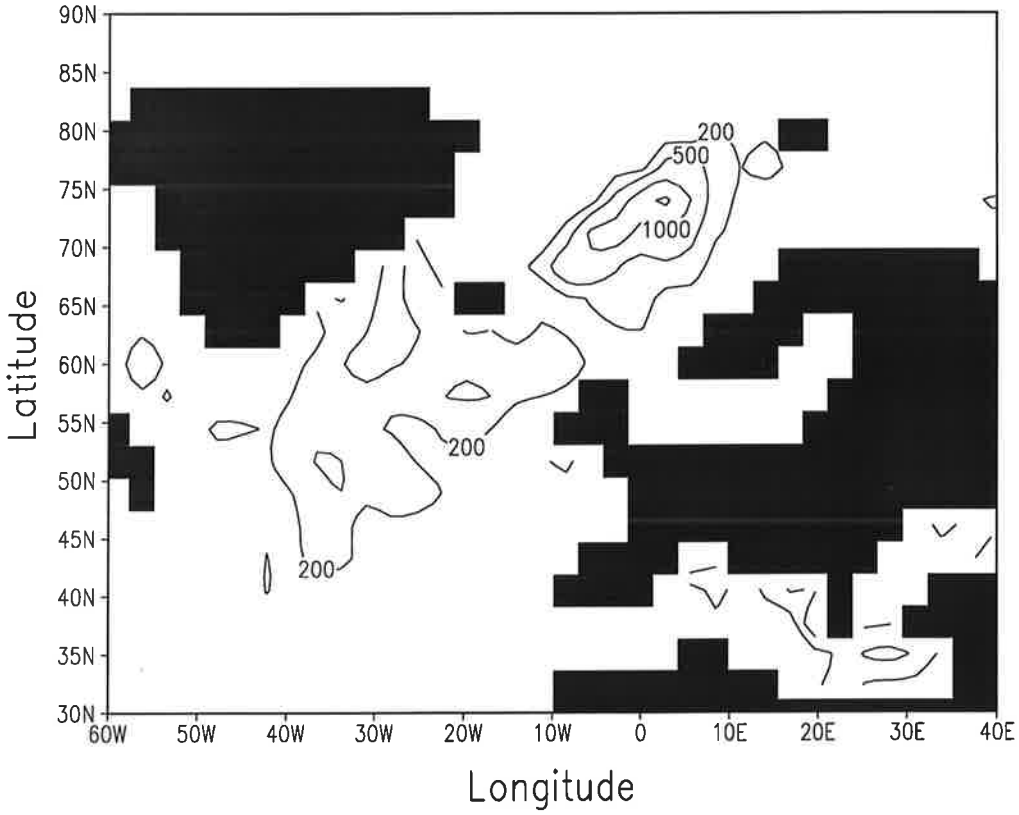

Fig. 3. Annual mean convective depth (m) in the northern North Atlantic.

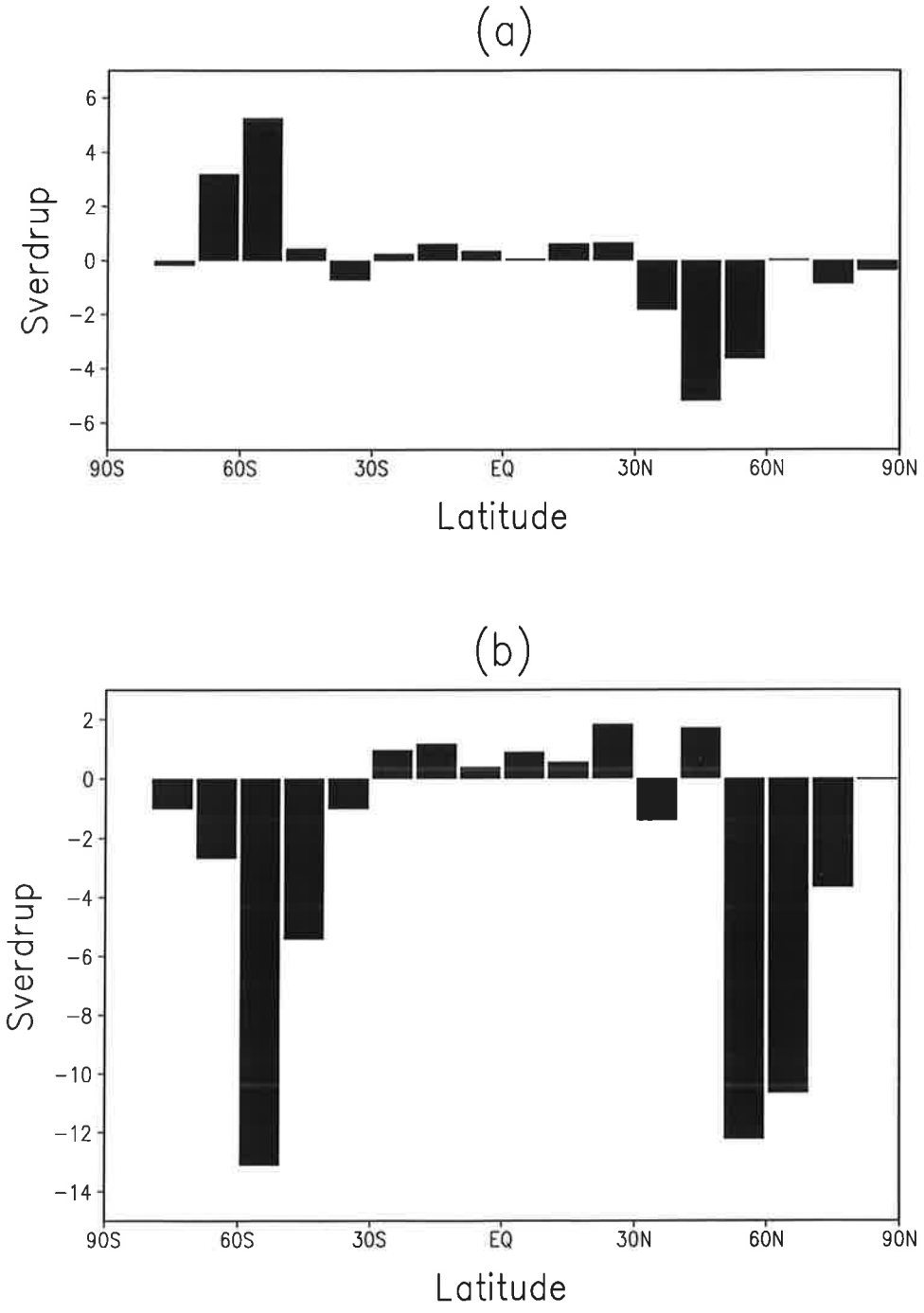

Fig. 4. Latitudinal distribution of inter-layer transport (Sv) in the Atlantic Ocean for (a) ML-to-UL, (b) DL-to-ML.

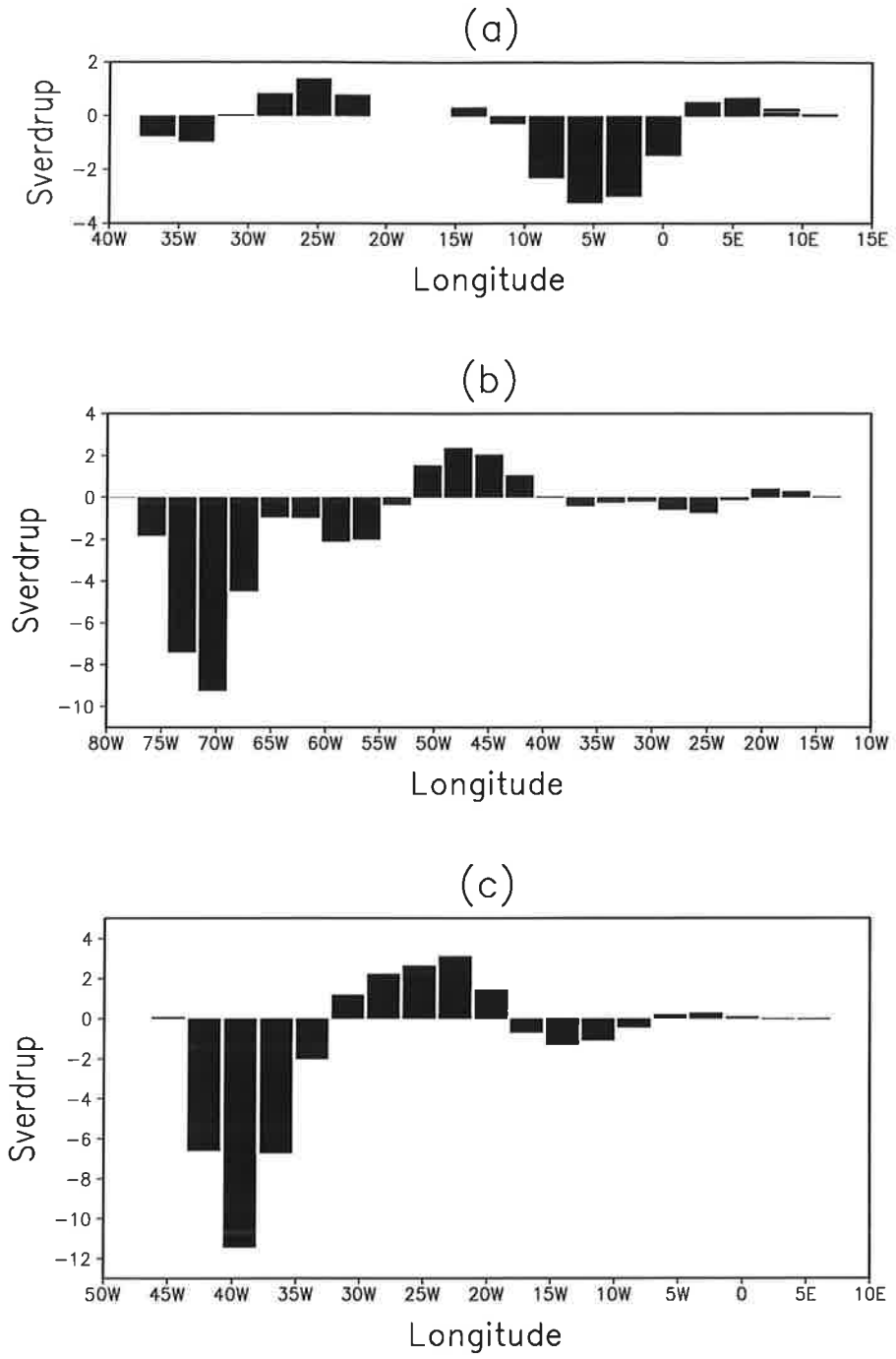

Fig. 5. Longitudinal distribution of DL-water meridional transport (Sv, positive value indicating northward transport) across the section along (a) 66°N, (b) 30°N, and (c) the equator in the Atlantic Ocean.

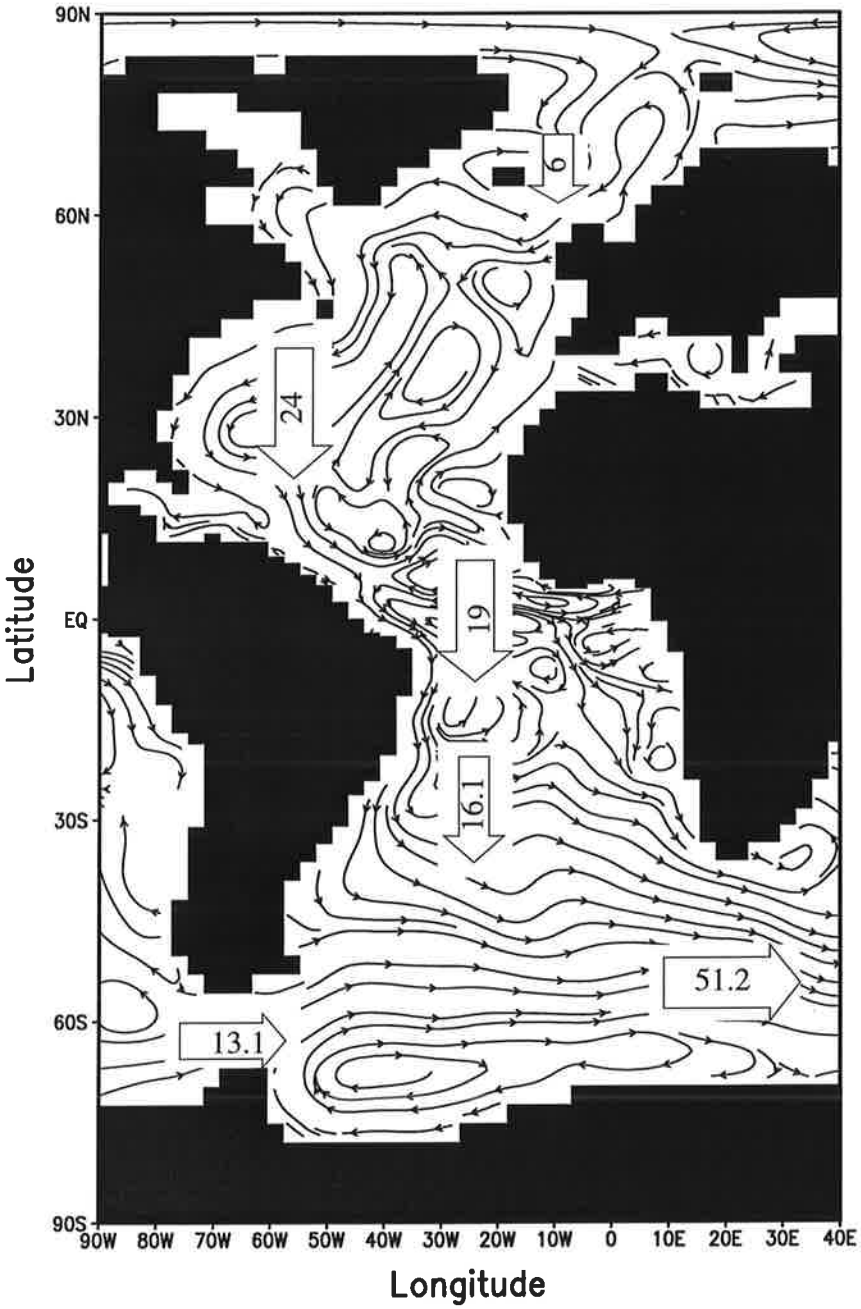

Fig. 6. Streamline of water mass flux in DL for the Atlantic Ocean. Figures indicate the net transports (Sv) across sections at 66°N, 31°N, the equator, 31°S, 70°W and 20°E respectively.

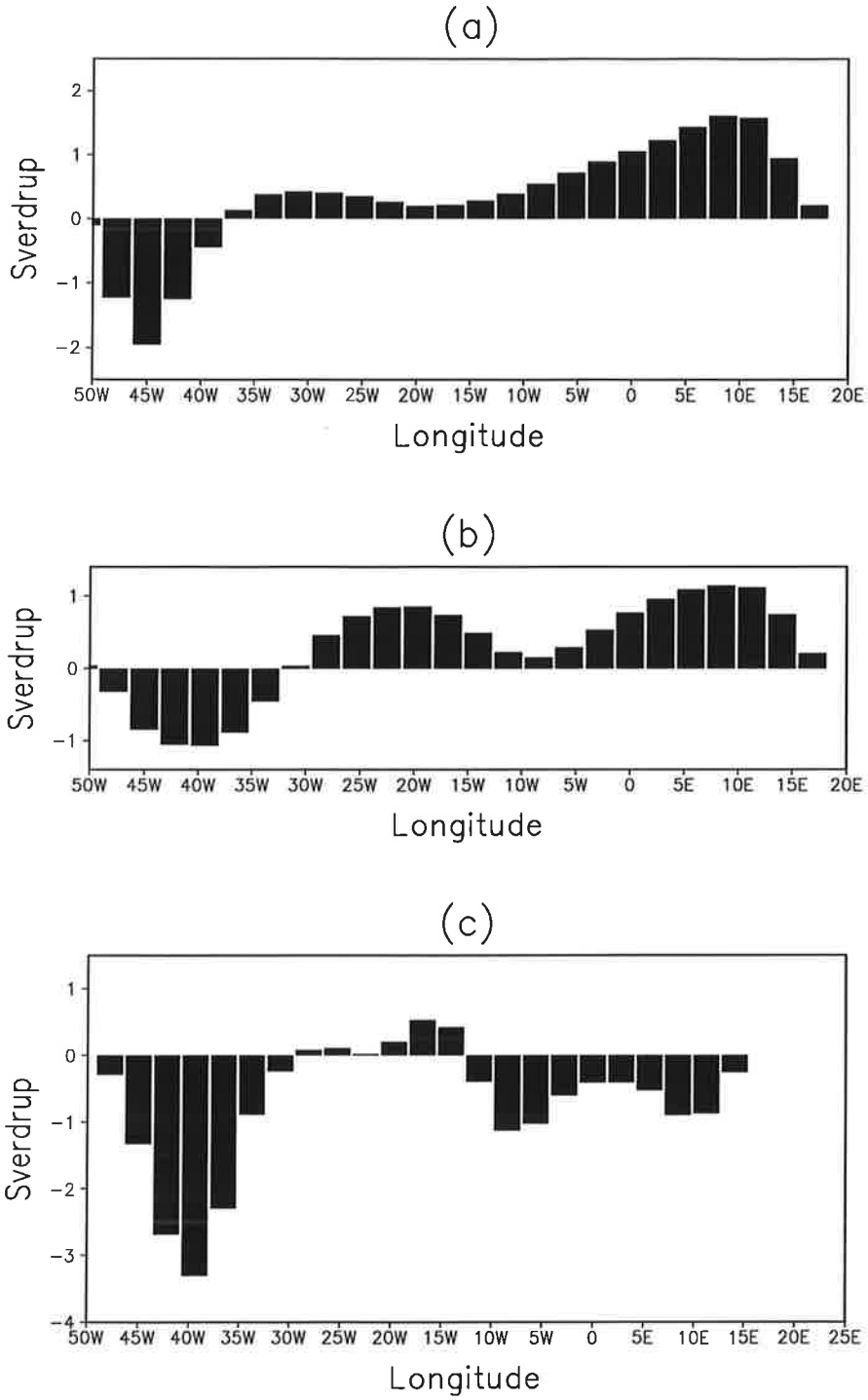

Fig. 7. Longitudinal distribution of meridional transport (Sv, positive value indicating northward transport) across the section along 31°S in the Atlantic Ocean for (a) UL, (b) ML, and (c) DL.

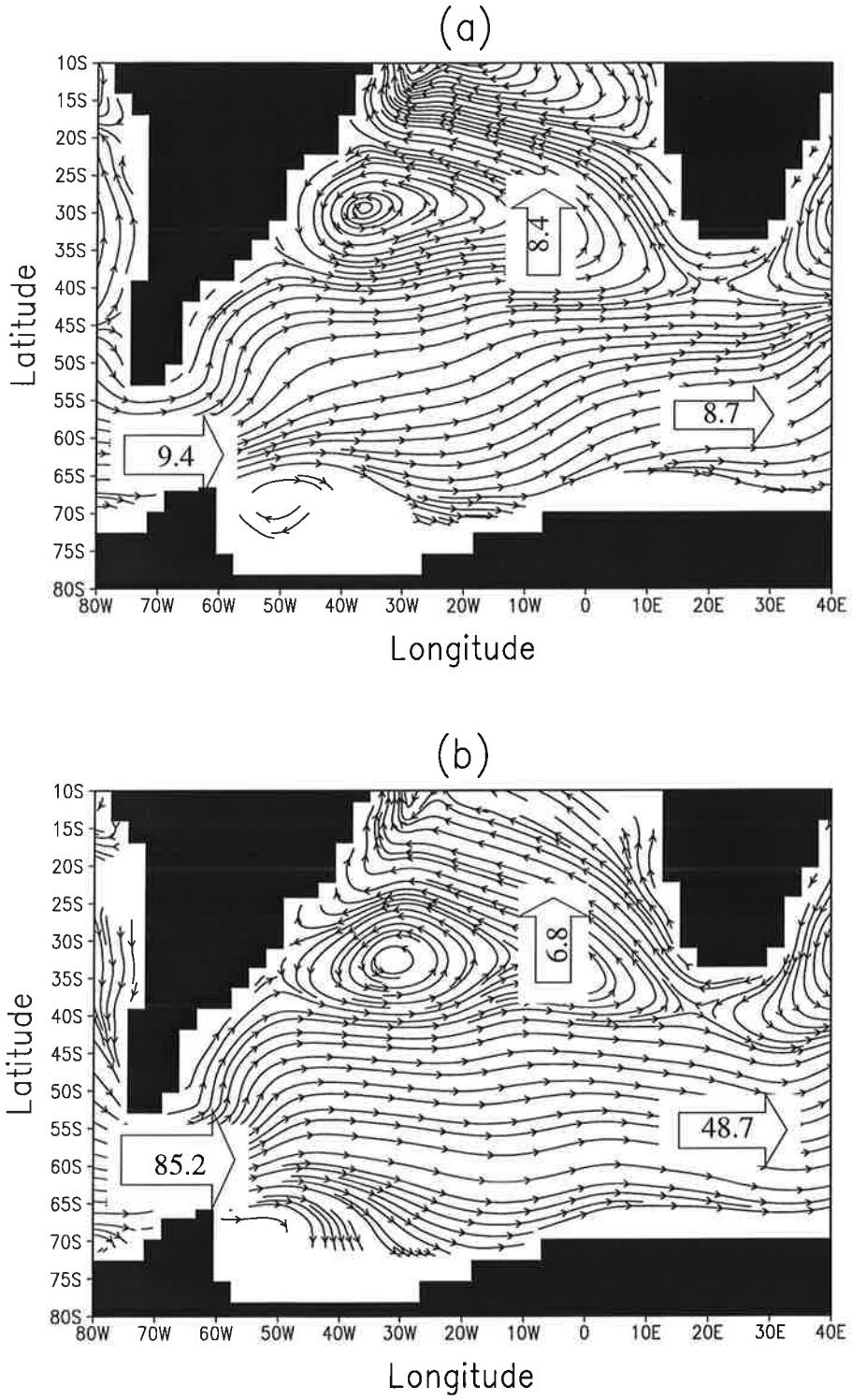

Fig. 8. Streamline of water mass flux in the South Atlantic Ocean for (a) UL, and (b) ML. Figures indicate the net transports (Sv) across sections at 70°W, 20°E and 31°S respectively.

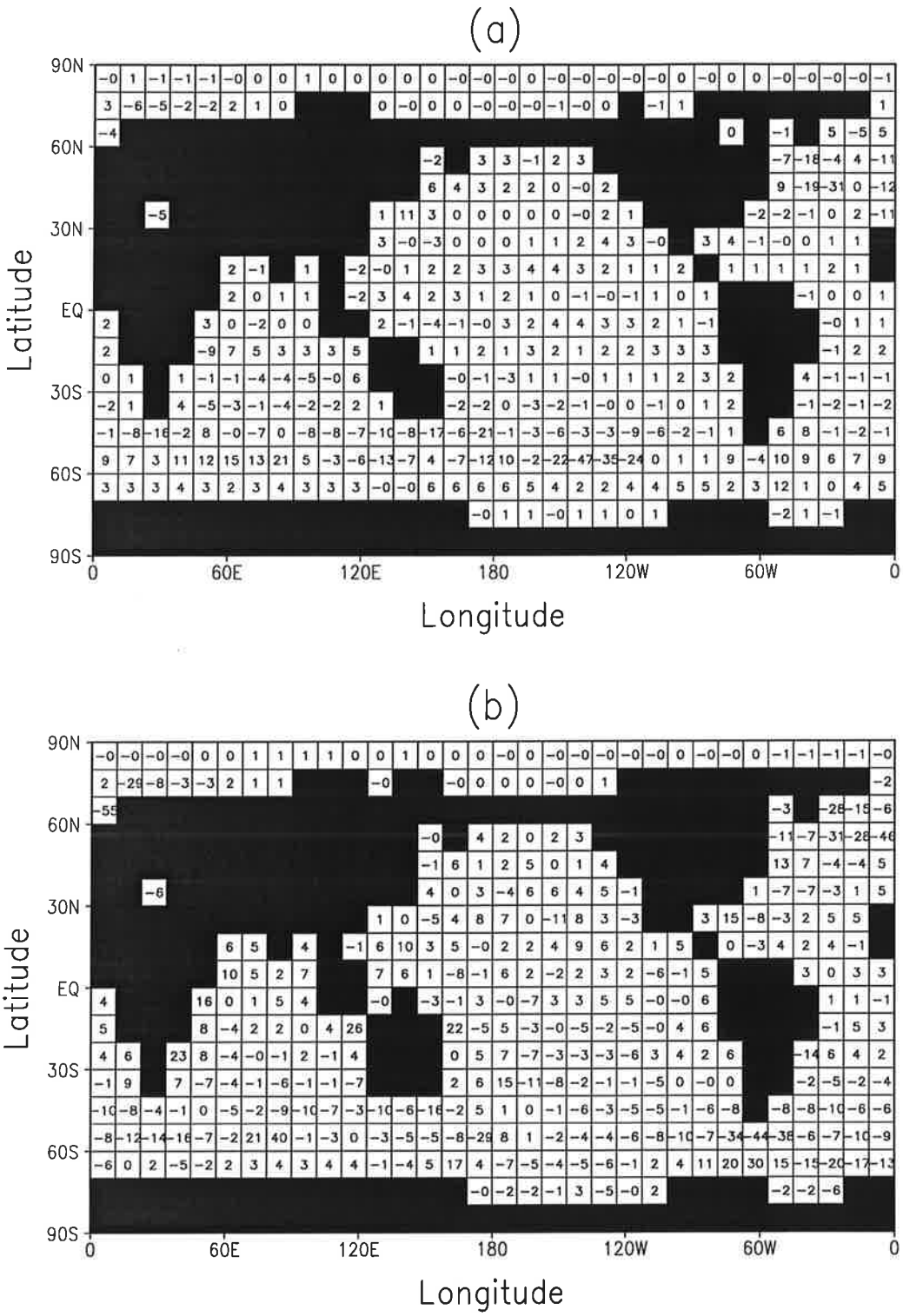

Fig. 9. Horizontal distribution of inter-layer transport summed in grid boxes of 11.25°x10° (Sv/10, positive indicating upward transport) for (a) ML-to-UL, and (b) DL-to-ML.

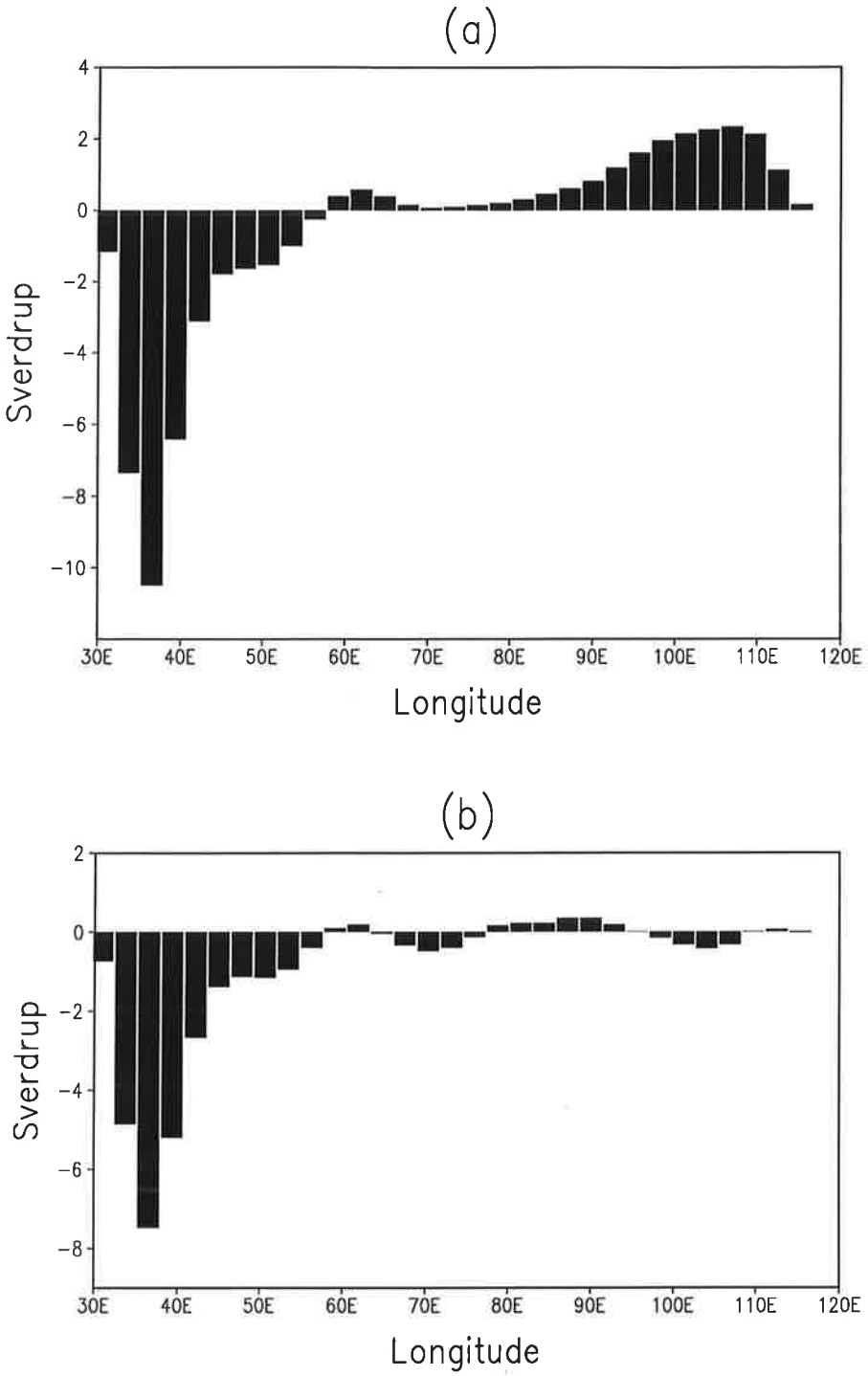

Fig. 10. Longitudinal distribution of meridional transport (Sv, positive value indicating northward transport) across the section along 31°S in the Indian Ocean for (a) UL, (b) ML.

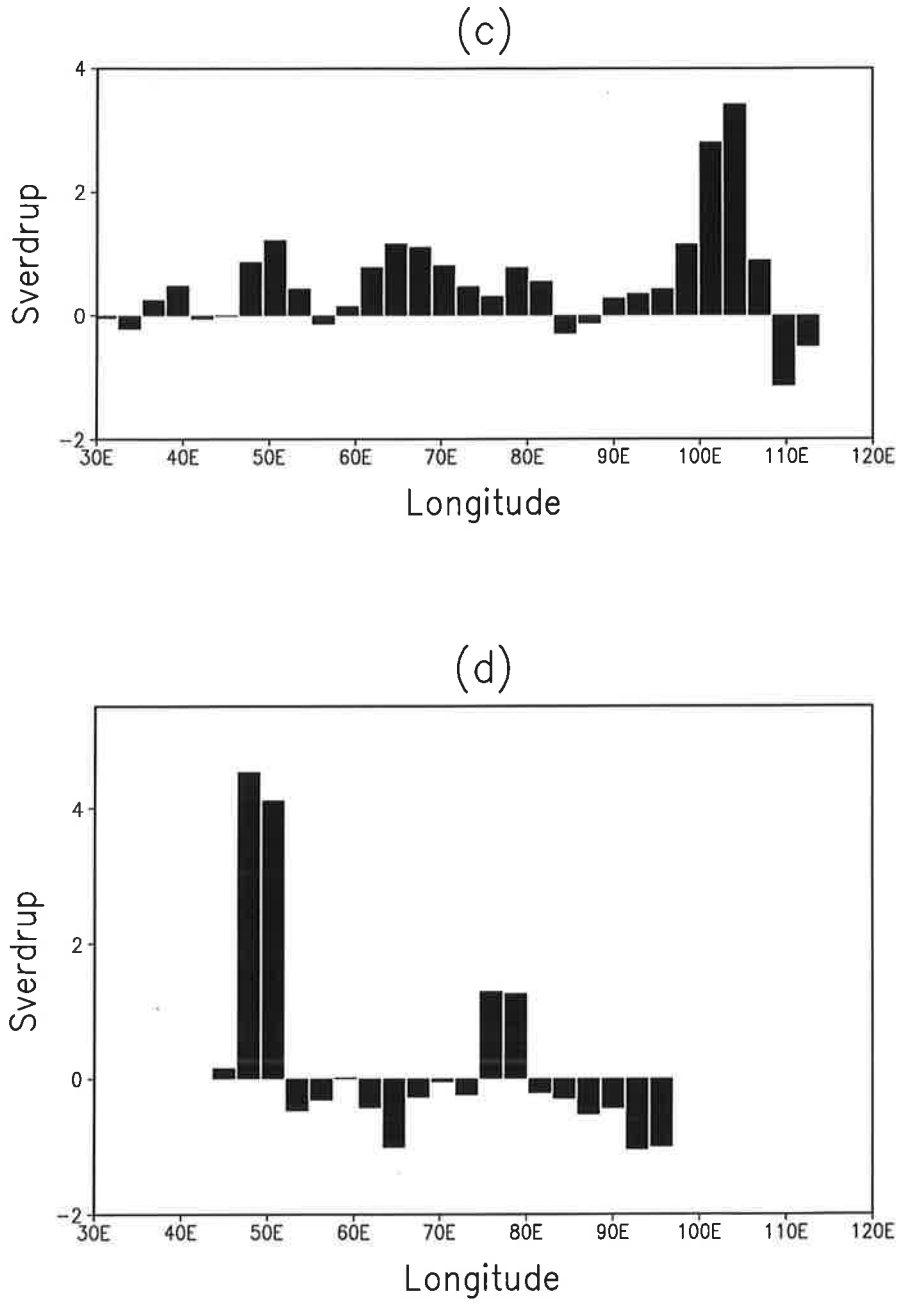

Fig. 10. (continued), (c) DL, and (d) northward transport of DL-water across the equator in the Indian Ocean.

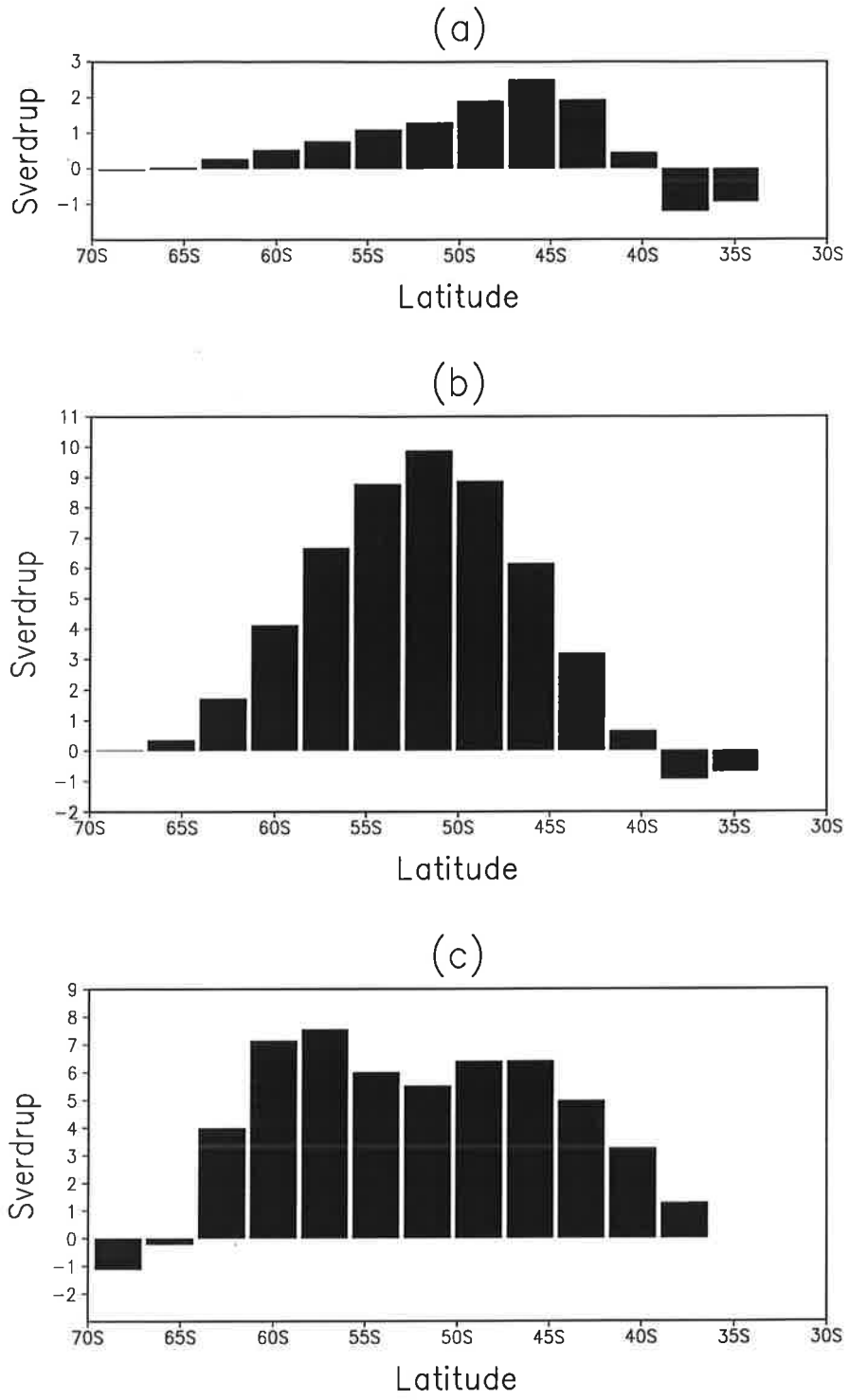

Fig. 11. Latitudinal distribution of eastward transport (Sv) across the section at 20°E for (a) UL, (b) ML, and (c) DL.

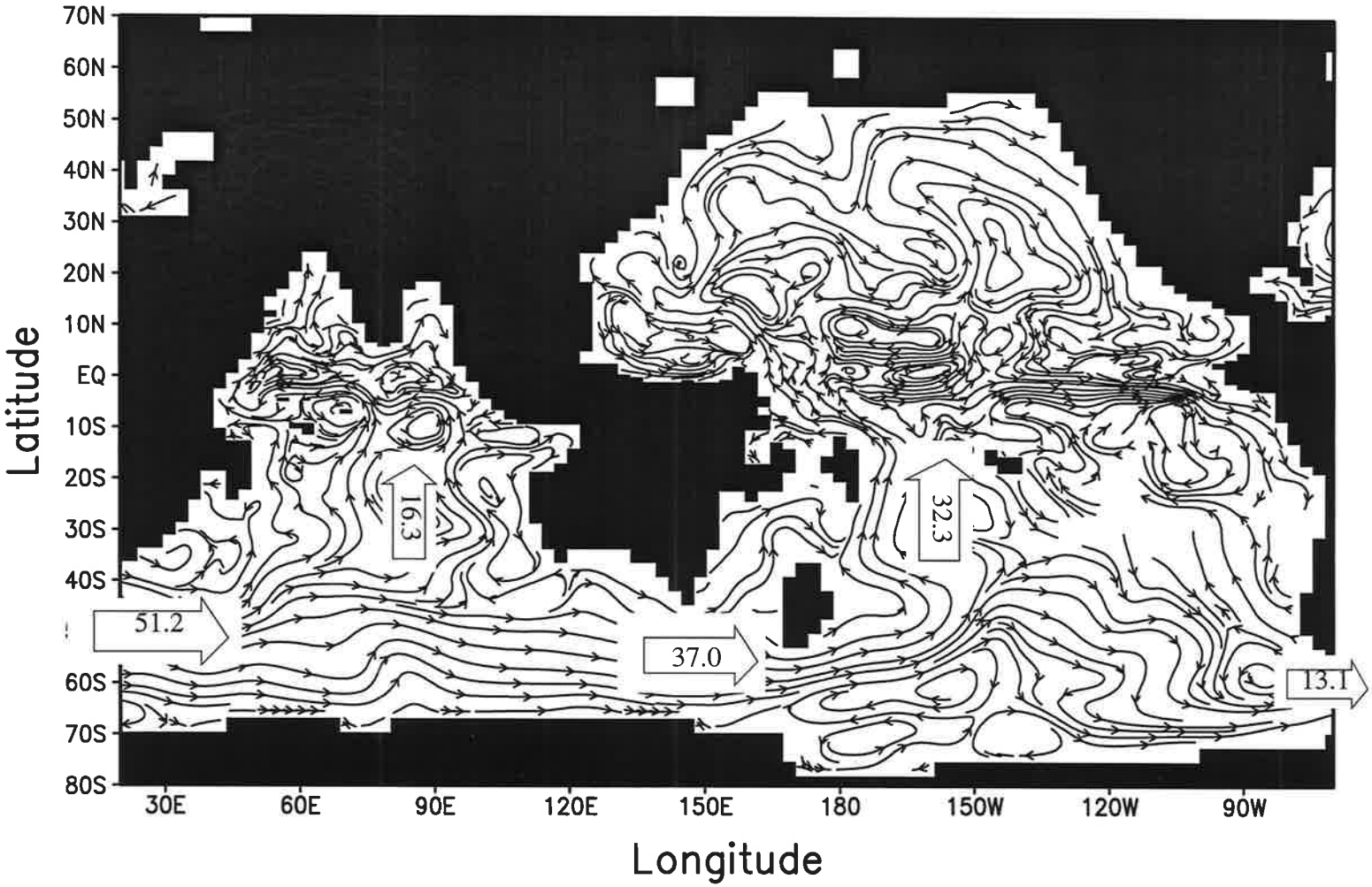

Fig. 12. Streamline of water mass flux in the Indian and Pacific Oceans for DL. Figures indicate the net transports across sections at 20°E, 150°E, 70°W and 31°S respectively

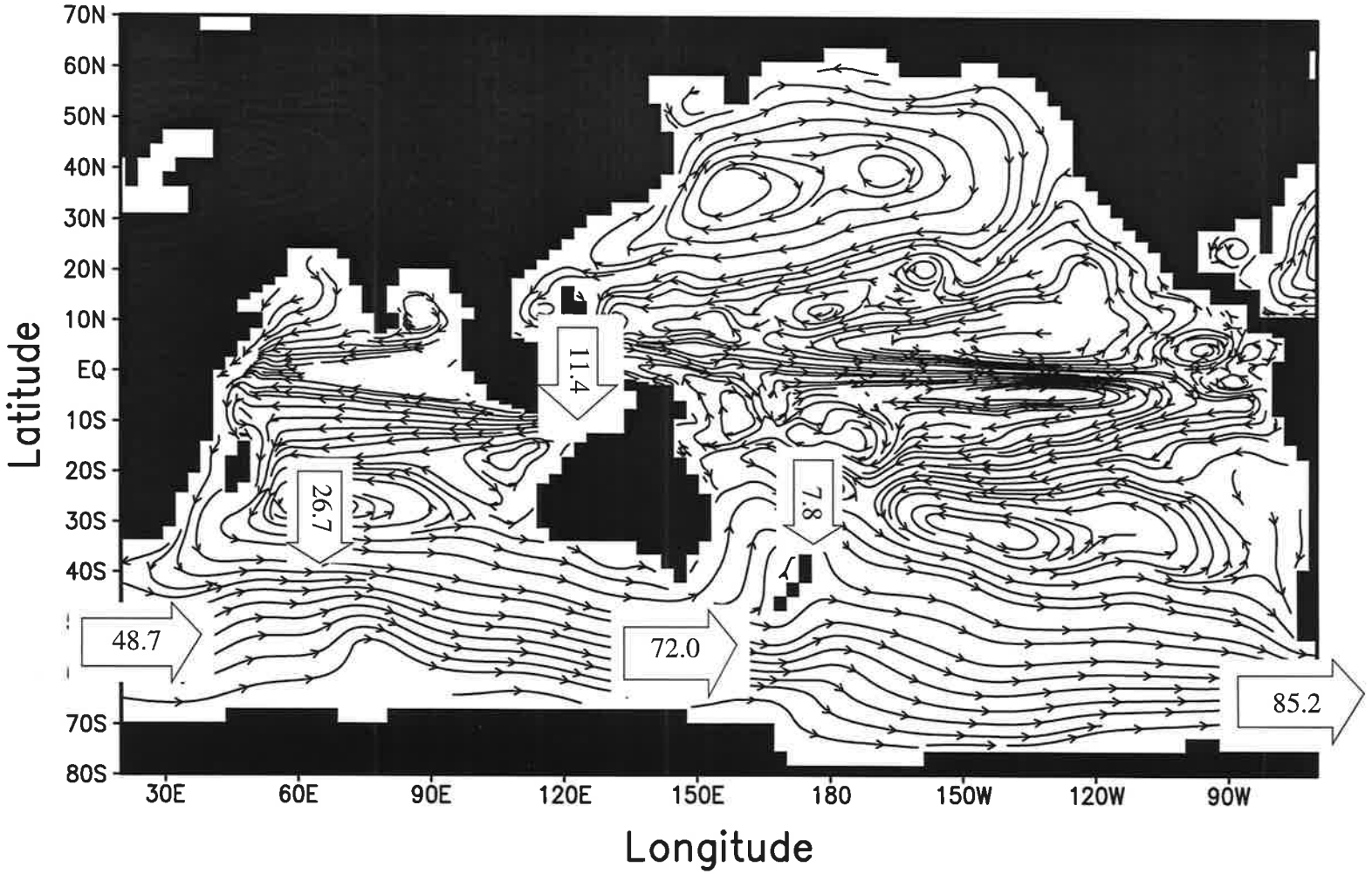

Fig. 13. Same as Figure 12 except for ML (and 11.4 Sv represents ML-water transport from Pacific to Indian Ocean through the Indonesian Passage).

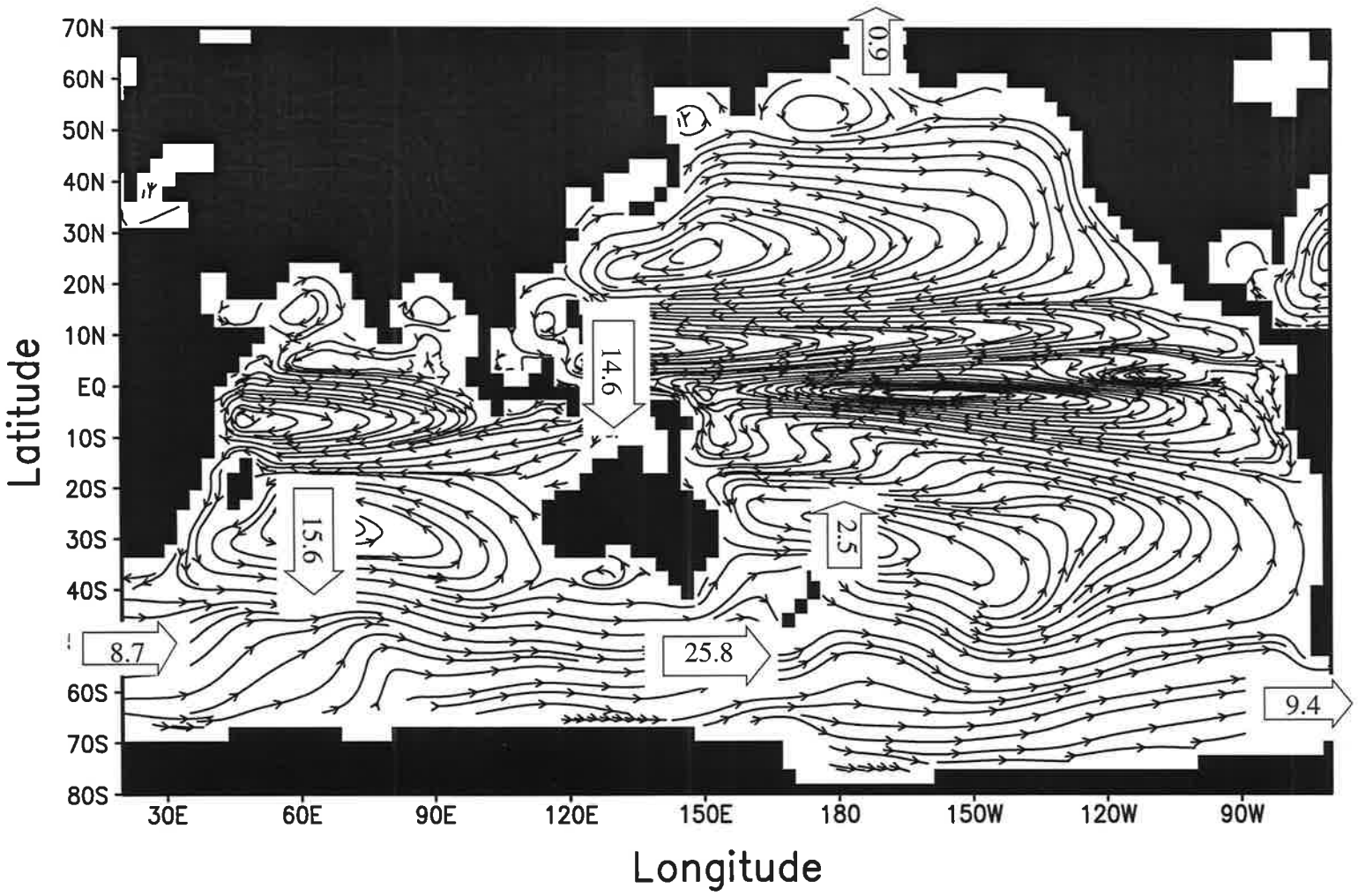

Fig. 14. Same as Figure 12 except for UL (and 14.6 Sv and 0.9 Sv represent the throughflows crossing the Indonesian Passage and Bering Strait respectively).

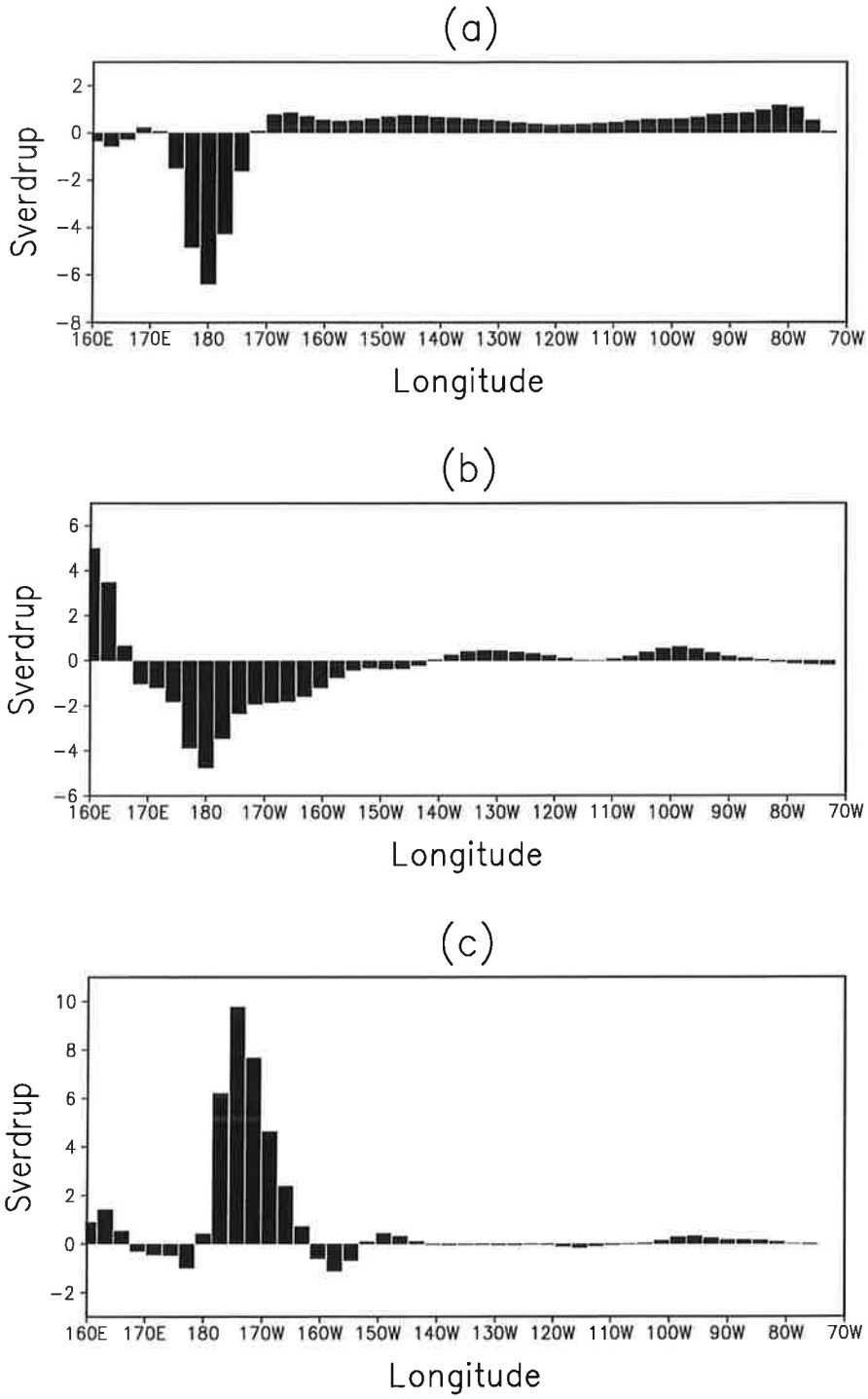

Fig. 15. Same as Figure 7 except for the Pacific Ocean.

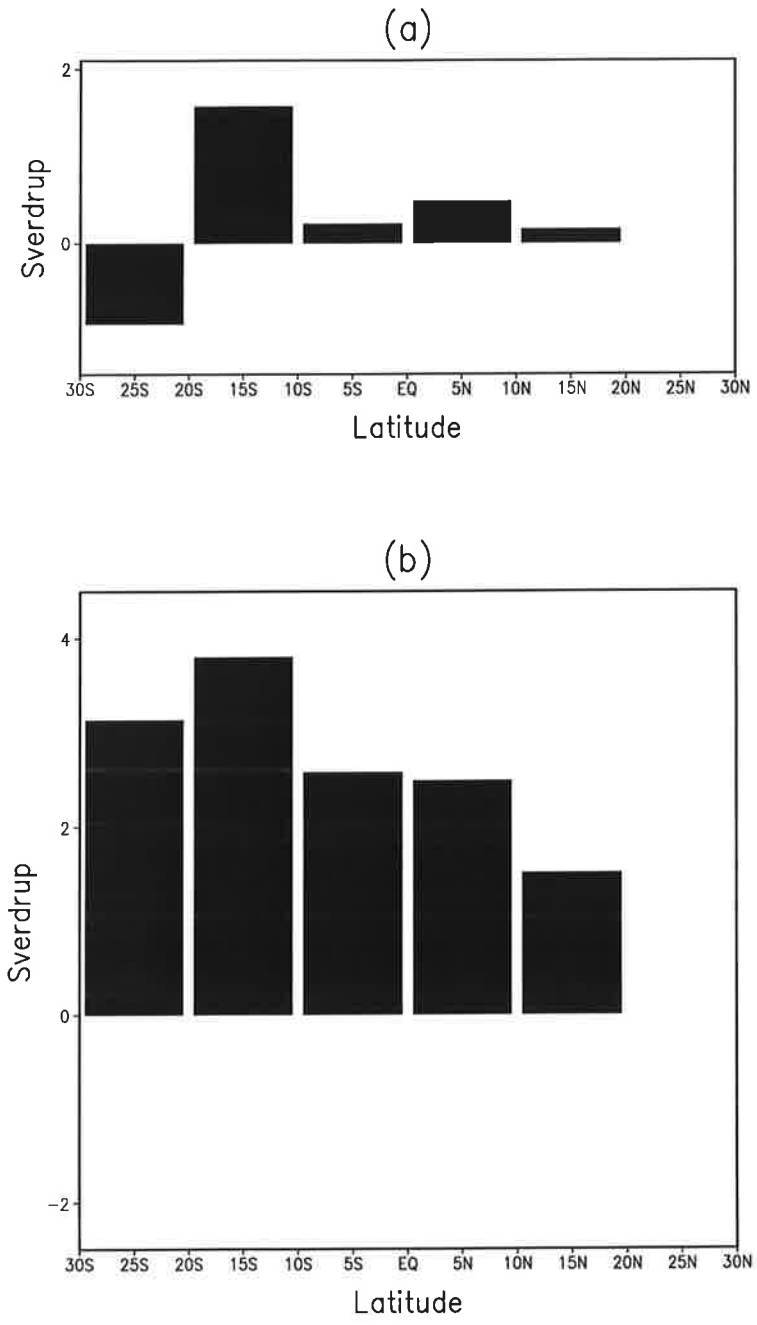

Fig. 16. Latitudinal distribution of inter-layer transport (Sv) in the Indian Ocean northward of 31°S for (a) ML-to-UL, and (b) DL-to-ML.

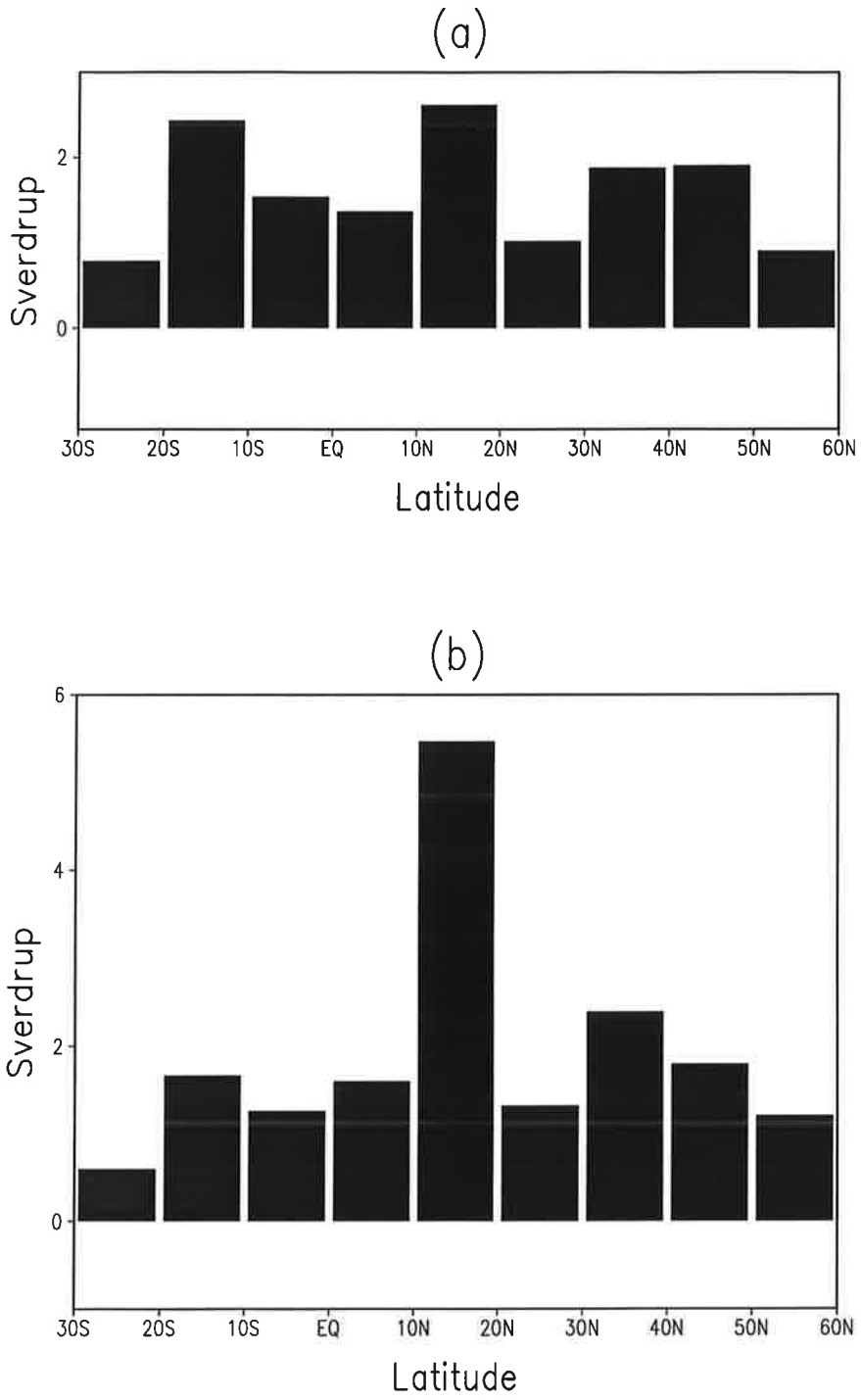

Fig. 17. Same as Figure 16 except for the Pacific Ocean.

REFERENCES

Arakawa A, Lamb VR (1977) Computational design of the basic dynamical processes of the UCLA General Circulation Model. Methods Comp Phys 17: 173-265.

Bacher A, Oberhuber JM (1996) Global coupling in the ECHAM4/OPYC3 atmosphere-sea ice-ocean GCM with annual mean flux correction restricted to heat and freshwater. Max-Planck Institute for Meteorology, Report (In preparation), Hamburg, FRG.

Bacher A, Oberhuber JM, Roeckner E (1996) ENSO dynamics and seasonal cycle in the tropical Pacific as simulated by the ECHAM4/OPYC3 coupled general circulation model. Clim Dyn (submitted).

Broecker WS (1987) The biggest chill. Nat Hist Mag 97: 74-82.

Broecker WS (1991) The great ocean conveyor. Oceanography 4: 79-89.

Bryan F (1986) High latitude salinity effects and interhemispheric thermohaline circulation. Nature 323: 301-304.

Bryan K, Lewis LJ (1979) A water mass model of the World Ocean. J Geopys Res 84: 2503-2517.

Cox MD (1989) An idealized model of the world Ocean. Part I: The global scale water masses. J Phys Oceanogr 19: 1730-1752.

Gordon AL (1986) Interocean exchange of thermocline water. J Geopys Res 91: 5037-5046.

Gordon AL, Weiss RF, Smethie WM, Warner MJ (1992) Thermocline and intermediate water communication between the South Atlantic and Indian Oceans, J Geopys Res 97: 7223-7240.

England MH (1993) Representing the global-scale water masses in ocean general circulation models. J Phys Oceanogr 23: 1523-1552.

England MH, Garcon VC (1994) South Atlantic circulation in a world ocean model. Ann Geophys 12: 812-825.

Haney RL (1971) Surface thermal boundary condition for ocean circulation models. J Phys Oceanogr 1: 241-248.

Hellermann S, Rosenstein M (1983) Normal monthly wind stress over the world ocean with error estimates. J Phys Oceanogr 13:1093:1104.

Hibler WD III (1979) A dynamic thermodynamic sea ice model. J Phys Oceanogr 9:815-846.

Killworth PD (1983) Deep convection in the world ocean. Rev Geopys and Space Phys 21: 1-26.

Macdonald AM (1993) Property fluxes at 30S and their implications for the Pacific-Indian throughflow and global heat budget. J Geophys Res 98C: 6851-6868.

Maier-Reimer E, Mikolajewicz U, Hasselmann K (1993) Mean circulation of the LSG OGCM and its sensitivity to the thermohaline forcing. J Phys Oceanogr 23: 731-757.

Manabe S, Stouffer RJ, Spelman MJ, Bryan K (1991) Transient response of a coupled ocean-atmosphere model to graduate changes of atmospheric CO_2. Part I: Annual mean response. J Clim 4: 785-818.

Oberhuber JM (1988) An atlas based on the 'COADS' data set: The budgets of heat, buoyancy and turbulent kinetic energy at the surface of the global ocean. Max-Planck Institute for Meteorology, Report No 15, Hamburg, FRG.

Oberhuber JM (1992) The OPYC Ocean General Circulation Model. Deutsches Klimarechenzentrum GmbH, Technical Report No.7, Hamburg, FRG.

Oberhuber JM (1993a) Simulation of the Atlantic circulation with a coupled sea ice-mixed layer-isopycnal general circulation model. Part I: Model description. J Phys Oceanogr 23: 808-829.

Oberhuber JM (1993b) Simulation of the Atlantic circulation with a coupled sea ice-mixed layer-isopycnal general circulation model. Part I: Model description. J Phys Oceanogr 23: 830-845.

Reid JL (1981) On the mid-depth circulation of the World Ocean. in Evolution of Physical Oceanography, MIT Press, 623pp.

Rintoul SR (1991) South Atlantic interbasin exchange. J Geophys Res 96: 2675-2692.

Roeckner E, Arpe K, Bengtsson L, Brinkop S, Dümenil L, Esch M, Kirk E, Lunkeit F, Ponater M, Rockel B, Sausen R, Schlese U, Schubert S, Windelband M (1992) Simulation of the present-

day climate with the ECHAM model: Impact of model physics and resolution. Max-Planck-Institute for Meteorology, Report No. 93, Hamburg, FRG.

Roeckner E, Arpe K, Bengtsson L, Christoph M, Claussen M, Dümenil L, Esch M, Giorgetta M, Schlese U, Schulzweida U (1996) The Max Planck Institute for Meteorology fourth-generation atmospheric general circulation model ECHAM4: Model description and climatology, In preparation.

Roeckner E, Oberhuber JM, Bacher A, Christoph M, Kirchner I (1996) ENSO variability and atmospheric response in a global coupled atmosphere-ocean model. Clim Dyn (accepted).

Sausen R, Barthel K, Hasselmann K (1988) Coupled ocean-atmosphere models with flux correction. Clim Dyn 2: 145-163.

Schmitz WJ (1995) On the interbasin-scale thermohaline circulation. Rev Geophysics 33: 151-173.

Semtner AJ, Chervin RM (1992) Ocean general circulation from a global eddy-resolving model. J Geopys Res 97: 5493-5550.

Toole JM, Warren BA (1993) A hydrographic section across the subtropical South Indian Ocean. Deep Sea Res 40: 1973-2019.

Toole JM, Polzin KL, Schmitz RW (1994) Estimates of diapycnal mixing in the abyssal ocean. Science 264: 1120-1123.

Wijffels SE, Schmitt RW, Bryden HL, Stigebrandt A (1992) Transport of freshwater by the Oceans. J Phys Oceanogr 22:155-162.

Wunsch C, Hu D, Grant B (1983) Mass, heat, salt, and nutrient fluxes in the South Pacific Ocean. J Phys Oceanogr 13: 725-753.

Zhang S, Greabatch RJ, Lin CA (1993) A reexamination of the polar halocline catastrophe and implications for coupled ocean-atmosphere modelling. J Phys Oceanogr 23: 287-299.

Zhang XH, Chen KM, Jin XZ, Lin WY, Yu YQ (1994) Simulation of thermohaline circulation with a twenty-layer oceanic general circulation model. Theor Appl Clim (to be published).